Quaternary Science Reviews 260 (2021) 106930

Contents lists available at ScienceDirect

Quaternary Science Reviews

journal homepage: www.elsevier.com/locate/quascirev

Prehistoric human response to climate change in the Bonneville basin, western North America: The Bonneville Estates Rockshelter radiocarbon chronology

Ted Goebel [a, *], Bryan Hockett [b], David Rhode [c], Kelly Graf [a]

[a] Center for the Study of the First Americans, Department of Anthropology, Texas A&M University, College Station, TX, USA
[b] Nevada State Office, U.S. Department of Interior Bureau of Land Management, Reno, NV, USA
[c] Desert Research Institute, Reno, NV, USA

ARTICLE INFO

Article history:
Received 24 February 2021
Received in revised form
31 March 2021
Accepted 31 March 2021
Available online 21 April 2021

Handling Editor: Donatella Magri

Keywords:
Climate and humans
Hunter-gatherers
Archaeology
Great Basin
Bonneville basin

ABSTRACT

The extent to which long-term climate change has influenced cultural evolution among hunter-gatherers has long been debated. In the Great Salt Lake desert (USA), a detailed record of paleoenvironmental change has been developed for the last 15,000 years, but a similarly complete chronicle of human occupation and adaptation is less secure. Here, we report and analyze one of the largest datasets (n = 247) of radiocarbon ages yet amassed from a single archaeological site in the Americas — Bonneville Estates Rockshelter, Nevada — to investigate human-environment interaction in this desert setting since 13,000 years ago. Results show a striking consistency in human-occupation intensity and oscillations between cool, mesic and warm, arid climate, specifically high occupation intensity during relatively cool times, and low intensity — even abandonment — during extended periods of drought. The ultimate outcome is a clear case of how long-term oscillations in climate can repeatedly motivate change in foraging societies in a marginal environmental setting.

1. Introduction

Numerous studies have demonstrated that climate change, whether abrupt or gradual, can prompt adjustments in human demography, technology, subsistence, and settlement. Certainly, agricultural and industrial societies have been impacted in this way (e.g., Benson et al., 2009; Kennett et al., 2012), but foraging societies, too, have felt the abrupt and cumulative effects of climate and environmental change, because so much of their success depends on the abundance, distribution, and predictability of wild plant and animal resources (e.g., Louderback et al., 2011; Kelly et al., 2013; Tallavaara et al., 2015). Nevertheless, proving a strong correlation between long-term paleoenvironmental and culture change has been difficult, given poorly constrained chronologies of such events in prehistory (cf. Zimmerman and Wahl, 2020), as well as equifinality in interpreting variation in the archaeological record.

In examining the consequences of long-term climate and environmental change on prehistoric societies in the Great Basin, USA, a region that has contributed much to our understanding of climate history since the late Pleistocene (e.g., Benson et al., 1990; Curry, 1990; Oviatt et al., 1992; Hostetler et al., 1994; Oviatt, 1997; Benson et al., 1997; Lupo and Schmitt, 1997; Benson et al., 2007; Lyle et al., 2012; Lachniet et al., 2014; McGee et al., 2018), we confront the chronological problem by developing a high-resolution history of human use of a single archaeological site — Bonneville Estates Rockshelter, Nevada — testing the hypothesis that during the past 13,000 calendar years, human occupation of this remarkable place was interwoven with regional environmental conditions and global climatic trends. The immediate result is one of the most thorough and protracted archaeological-site chronologies in the Americas, a sequence of 247 individual radiocarbon ages spanning from before 13,000 calendar years ago (cal yr BP) to historic times (< 100 cal yr BP). The ultimate outcome is a clear case of how long-term oscillations in climate can repeatedly motivate change in foraging societies in a marginal environmental setting.

Bonneville Estates Rockshelter (CRNV-11-4893) is located in the western Bonneville basin (a major component of the Great Salt Lake Desert) of northeast Nevada and northwest Utah, 6 km west of the

* Corresponding author.
E-mail address: goebel@tamu.edu (T. Goebel).

https://doi.org/10.1016/j.quascirev.2021.106930
0277-3791/

Nevada-Utah border and ~30 km south of the city of West Wendover, Nevada (Fig. 1). Lying at an elevation of ~1585 m asl, the site is perched upon the highest shoreline of Pleistocene Lake Bonneville. This is a mid-elevation setting of the Great Basin Desert, 300 m above the western Bonneville basin's playa floor and 1300 m below the crest of the nearby Goshute Mountains. The traditional inhabitants of the region, Gosiute Shoshone foragers, subsisted on a variety of wild plant and animal resources: marsh plants and waterfowl in well-watered playa margins; seeds of a variety of desert grasses and shrubs as well as cacti and jackrabbits (*Lepus californicus*) in low- and mid-elevation settings; nuts of pinyon pine (*Pinus monophylla*) in mid-to high-elevation settings; and sage-grouse (*Centrocercus urophasianus*) and artiodactyls including pronghorn antelope (*Antilocapra americana*), mountain sheep (*Ovis canadensis*), and mule deer (*Odocoileus hemionus*), normally at elevations above Bonneville Estates (Chamberlin, 1911; Steward, 1938). The broad elevational (and seasonal) distribution of these resources contributed significantly to high residential mobility, as recorded both ethnographically and archaeologically (Steward, 1938; Kelly, 2001).

Today and throughout much of prehistory, Bonneville Estates has straddled an important ecotone — the transition from upland-sagebrush (*Artemisia* sp.) to lowland-shadscale (*Atriplex* sp.) desert-shrub communities (Fig. 3). From this ecotonal vantage, the rockshelter is well-positioned for measuring variation in prehistoric occupation intensity and resource use in response to changes in effective temperature and moisture. During cooler, wetter episodes of the latest Pleistocene and Holocene, relatively abundant sagebrush, grass, and conifer communities spread downslope to near the rockshelter's elevation, locally promoting relatively diverse and abundant populations of flora and fauna, many species of which were economically important to humans. Conversely, during hotter and drier periods, as effective moisture and water became scarce, xerophytic shrubs of the Amaranthaceae family spread from downslope of the rockshelter, replacing sagebrush, grass, and conifers and leading to a local decline in economically-important flora and fauna. Human subsistence carried out from the rockshelter, as well as the timing and frequency of visits, would have been affected as well. We predict that during cooler, wetter periods, human populations were active locally and the rockshelter served as an attractive base for human subsistence and settlement; conversely, during hotter, drier periods, local human groups visited the area less frequently and their use of the rockshelter waned. During extreme, prolonged drought events, we expect that occupation may have ceased altogether for centuries or even millennia, given that even during more mesic times, the nearest perennial sources of water are 8 km away.

Large-scale excavation of Bonneville Estates Rockshelter occurred between 2000 and 2009 (Fig. 4), during which we dug an area of ~52 sq m through a series of Holocene and late-Pleistocene deposits to a maximum depth of 3 m. The site contains a well-stratified record of human occupation (Fig. 5). Its earliest fire-

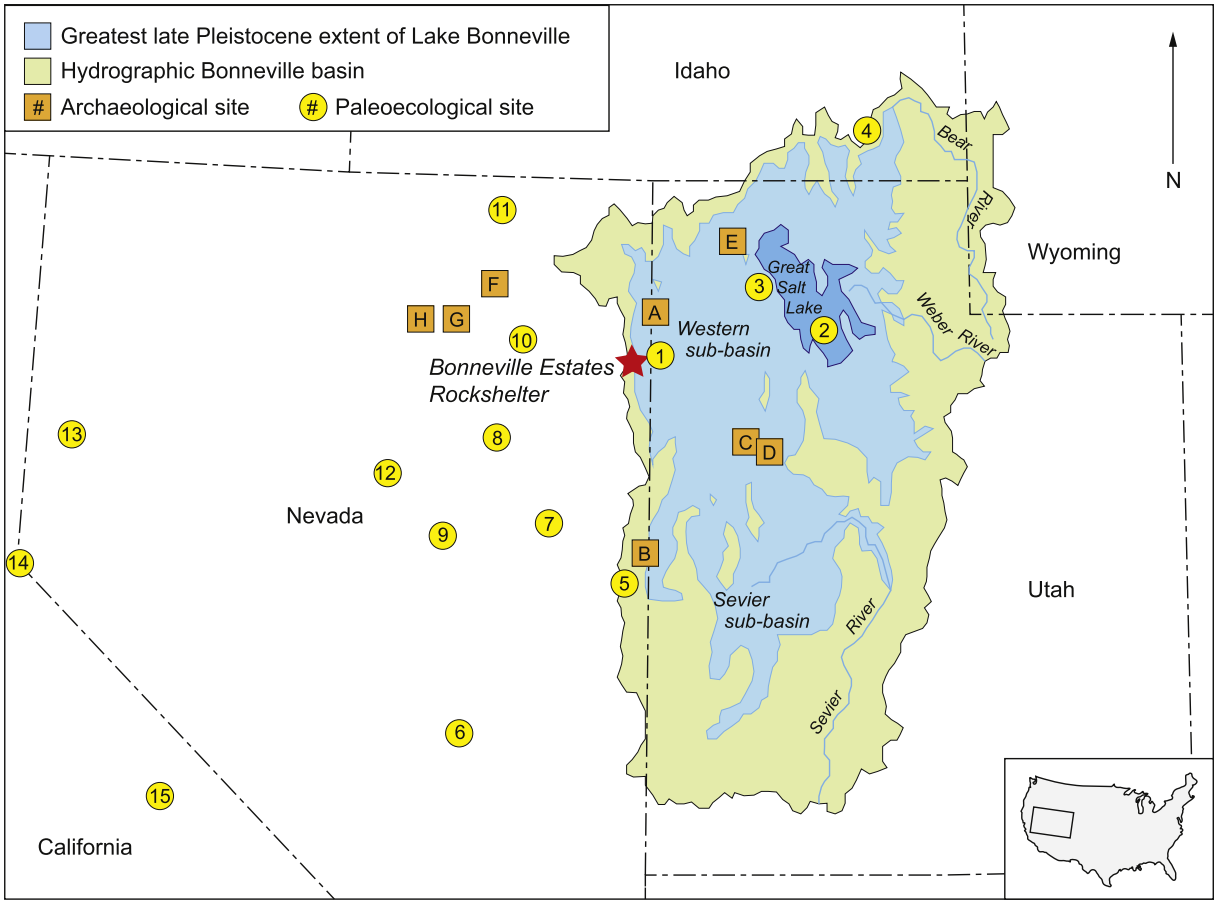

Fig. 1. Map of interior western North America, showing locations of Bonneville Estates Rockshelter (star) in relation to the Bonneville basin, Pleistocene Lake Bonneville, and other archaeological and paleoecological sites mentioned in the text (A, Danger Cave; B, Smith Creek Cave; C, Old River Bed; D, Camels Back Cave; E, Hogup Cave; F, Pie Creek Shelter; G, South Fork Shelter; H, James Creek Shelter; 1, Blue Lake marsh; 2, Great Salt Lake (GSL) 96+ core; 3, Homestead Cave; 4, Red Rock Pass; 5, Lehman Cave; 6, Leviathan Cave; 7, Stonehouse Meadow; 8, Newark Valley Pond; 9, Kingston Meadow; 10, Ruby Marshes; 11, Mission Cross Bog; 12, Gund Ranch; 13, Pyramid Lake; 14, Lake Tahoe; 15, Mono Lake). (For interpretation of the references to colour in this figure legend, the reader is referred to the Web version of this article.)

hearth features date to ~13,000 cal yr BP, and its latest, to just a few centuries ago. Stratigraphically, 20 distinct geological layers have been identified, generally a series of silt-and-rubble deposits (*éboulis*) interdigitated with organic-rich cultural deposits. This stratification resulted from alternating episodes of eolian sediment deposition and ceiling-rock fall versus the accumulation of well-preserved organic material from the activities of humans, woodrats (*Neotoma* sp.), raptors, and other animals. The remarkable organic preservation is due to the rockshelter's arid setting and a lack of interior moisture.

Based primarily on variation in bifacial-point form, we grouped the rockshelter's cultural layers into eight archaeological components correlating to the region's major phases of prehistory (Fig. 2; following Elston and Budy, 1990; Hockett and Morgenstein, 2003; McGuire et al., 2004; Hildebrandt et al., 2016; Hockett and Goebel, 2019). Boundary ages as well as bifacial-point forms for each phase are presented in Fig. 2. Most (but not all) component boundaries also correlate to stratigraphic changes in the record, for example transitions between organic-rich and eolian deposits.

In nine years of excavation at Bonneville Estates Rockshelter, we encountered and mapped 167 archaeological features, including 156 hearths, 8 pits, 2 mats, and 1 large pile of Indian-ricegrass (*Eriocoma hymenoides*) seed and chaff. Here we present radiocarbon ages on 151 of the hearths, 7 of the pits, and the single Indian-ricegrass feature, as well as a variety of other organic materials of cultural origin (e.g., human coprolites and perishable artifacts), together resulting in a chronology of 247 radiocarbon ages (Table S1). This constitutes one of the largest series of radiocarbon ages from a single archaeological site in the Western Hemisphere (cf. Martindale et al., 2016), providing one of the world's most chronologically comprehensive and precise single-site archives of human activity spanning the last 13,000 calendar years. Here we present that chronology and demonstrate its relationship to regional paleoenvironmental trends and global climate change.

2. Materials and methods

Throughout this report, we discuss time in cal yr BP; however, in instances where we present and critique individual radiocarbon ages in this section, we present them in radiocarbon years ago (^{14}C yr BP), collating them with the primary date list presented in Table S1.

2.1. Creation of the date list

As organic material was abundant in the excavations, we used accelerator (AMS) radiocarbon analysis to directly date all of the recognized cultural layers. Dating efforts centered on wood charcoal (of short-lived shrub species) from hearth features, not only because of the relative ease through which geochemists are able to pretreat and date burnt wood, but also because we interpret the hearths to represent specific human occupational events. We complemented the analysis of hearth charcoal with the direct dating of loose fibers extracted from perishable artifacts as well as gut-biome residue from desiccated human coprolites (Albush, 2010; Coe, 2020), and even sinew from the bindings of hafted stone tools (Smith et al., 2013). We generally avoided dating bone, except in the rockshelter's lowest deposits (Stratum 19), where cultural features and perishable artifacts were absent (Graf, 2007). Early in the project, as we developed a regimen for selecting radiocarbon samples, we unwittingly dated several samples of isolated charcoal as well as charcoal from dispersed features interpreted to represent 'dumps'. Not surprisingly, these mostly yielded discordant dates, reinforcing our strategy of exclusively dating charcoal from intact hearths.

The sample of 247 radiocarbon ages used in this analysis is presented in Table S1. In the table, details of each date are also provided, including lab number, provenience in the excavation, material dated, and instances where multiple ages were obtained on the same sample or the same archaeological feature. Generally, 168 (68.0%) are on hearth charcoal and provide ages for 151 distinct hearth features (of a total of 156 hearth features observed and documented in the excavation). Fifteen ages (6.1%) were from organics (charred and uncharred) recovered from 7 pit features (of 8 excavated); 13 (5.3%), from dispersed charcoal; 13 (5.3%), from fragments of baskets; 9 (3.6%), from fragments of twine; 8 (3.2%), from human coprolites; 8 (3.2%), from uncharred organics; 5 (2.0%), from charred organics; 5 (2.0%), from bone; 2 (0.8%), from point binding; and 1 (0.4%), from pronghorn hair. From the bottom upward in Table S1, the age of Component VIII (strata 20 and 19, 'Pre-Clovis' Phase) is defined by 6 stratigraphically consistent radiocarbon ages; Component VII (strata 18b–17b′, Dry Gulch Phase), by 51 consistent ages; Component VI (Stratum 17b, Wendover Phase), by 8 consistent ages; Component V (strata 17a-13, Pie Creek Phase), by 77 consistent ages; Component IV (Stratum 11, South Fork Phase), by 7 consistent ages; Component III (strata 9-3b, James Creek Phase), by 61 consistent ages; Component II (Stratum 3a, Maggie Creek Phase), by 16 consistent ages; and Component I (strata 2–1, Eagle Rock Phase), by 7 consistent ages.

Before conducting the Bayesian sequence analysis and summed-probability/kernel-density analysis, we scanned the date list for stratigraphically inconsistent ages. Of the 247 ages, only 13 (5.3%) were clearly out of stratigraphic sequence. Of these, 6 were dispersed charcoal, 3 were hearth charcoal, 2 were pit organics, 1 was binding affixed to an Eastgate bifacial point, and 1 was uncharred organics from a hearth. Given that these could have been re-deposited from original contexts by human or non-human agents, or in some cases they could represent materials (e.g., wood) taken by humans from pre-existing woodrat middens inside the rockshelter, we excluded them from the Bayesian sequence analysis (because of their inconsistent stratigraphic positions). However, we included all of them except the uncharred plant macrofossils in the summed-probability/kernel-density analysis, because they may still represent human activity, albeit displaced. In addition, five accepted ages came from disturbed contexts (Stratum 0 in Table S1) — either the modern surface of the rockshelter or deposits interpreted to represent looting activity. Although excluded from the Bayesian sequence analysis, these samples were included in the summed-probability/kernel-density analysis because they provide ages on unequivocal human-produced artifacts (baskets, twines, or coprolites).

Twenty-two of the 158 dated hearth and pit features yielded multiple radiocarbon dates (Table 1, S1; Fig. 6). Most of these were concordant ages that could be combined, but several of the features require discussion. Pit Feature 03.01/03.03 yielded three ages (985 ± 25, 1370 ± 60, and 1735 ± 25 ^{14}C yr BP) that are internally inconsistent. Stratigraphically, this pit was dug during the time of Stratum 2 of Component II (985 ^{14}C yr BP), and we interpret the older dates of 1370 and 1734 ^{14}C yr BP to represent older organics that fell into the pit when it was prehistorically dug into older deposits of strata 3a and 3b. Pit Feature 01.03/02.02/04.11/06.04 (Stratum 4 of Component III) was an extensive pit that yielded seven ages, six of which are consistent (between 1850 ± 25 and 2105 ± 25 ^{14}C yr BP) but the seventh, significantly older (3665 ± 30 ^{14}C yr BP), likely due to the redeposition of earlier charcoal into the pit as it was dug into earlier-aged (Stratum 9) deposits. Hearth Feature 07.07 (Stratum 14 of Component V) yielded a stratigraphically consistent age of 6150 ± 30 ^{14}C yr BP on charcoal and an inconsistent age of 4250 ± 25 ^{14}C yr BP on uncharred pine-nut hulls, the latter probably introduced by woodrats or some other non-

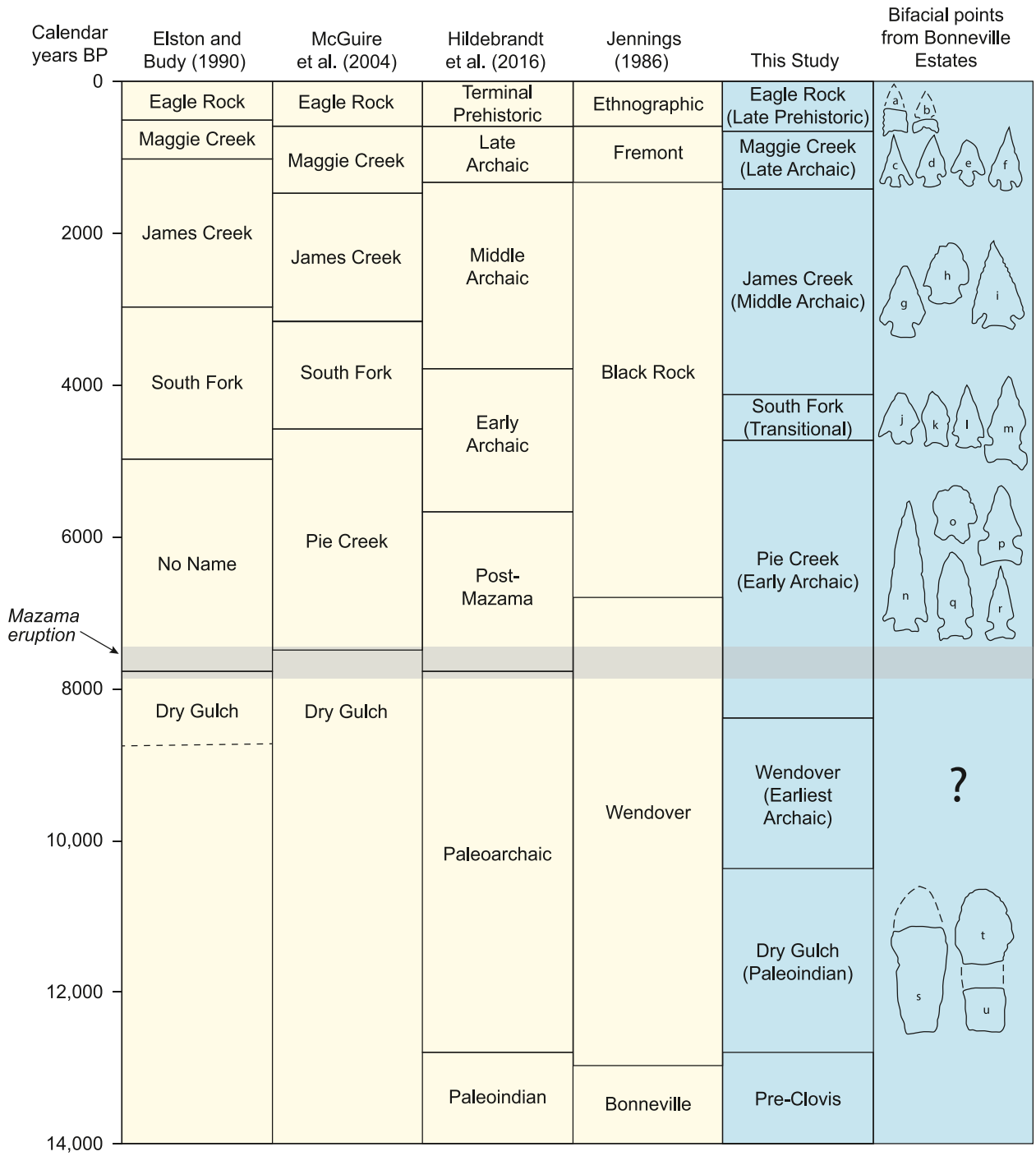

Fig. 2. Culture-history scheme for northeastern Nevada, used to organize the cultural layers at Bonneville Estates Rockshelter into meaningful cultural components (in blue) versus those previously developed chiefly through excavations at James Creek Shelter, South Fork Shelter, and Pie Creek Shelter in the upper Humboldt River valley of Nevada, and Danger Cave and Hogup Cave in the Bonneville basin of Utah (in yellow) (after Jennings, 1986; Elston and Budy, 1990; McGuire et al., 2004; Hildebrandt et al., 2016). The chrono-stratigraphic position of the widespread Mazama tephra is shown in gray. Also shown are outlines of representative bifacial-point forms (in blue) (a, Cottonwood triangular point; b, Desert side-notched point; c-f, Rosegate series (i.e., Rose Spring and Eastgate) points; g-i, Elko corner-notched points; j, Gatecliff point; k, Humboldt point; l, Dead Cedar corner-notched point; m, p-r, large side-notched points; n, Leppy Hills corner-notched point; o, Pinto point; s-u, fragments of Great Basin stemmed points. (For interpretation of the references to colour in this figure legend, the reader is referred to the Web version of this article.)

human agent and thus excluded from all analyses (as discussed above). These three features' consistent ages were respectively combined in the Bayesian and summed-probability/kernel-density analyses, while the ages on charcoal inconsistent with their stratigraphic contexts were excluded from the Bayesian sequence analysis but included in the summed-probability/kernel-density analysis, and ages on uncharred organics were excluded completely. Likewise, eight other features (02.01/03.04, D4-6-C-2/C-3, 01.08/05.01, C4-9-C-6, C6-8-C-1/C-2/D6-8-C01, 09.01a/b, 07.12, and D4-10-C-7b/D5-10-C-8a/8d) yielded multiple ages that were concordant stratigraphically but statistically so far apart that we could not combine them in the Bayesian sequence model

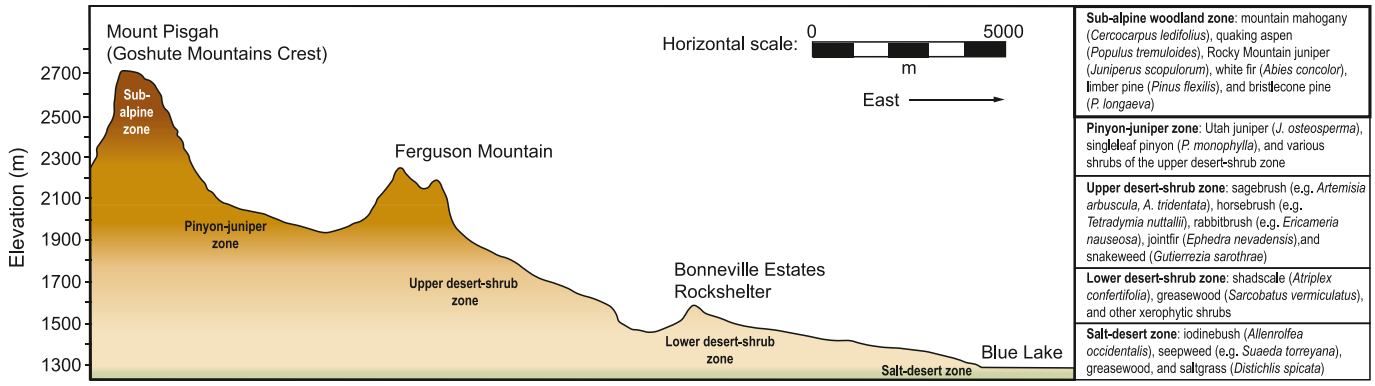

Fig. 3. Topographic cross section of area outside Bonneville Estates Rockshelter, from the crest of the Goshute Mountains (left) to the western Bonneville basin's playa floor (right). About 300 m lower in elevation and 8 km east of the rockshelter is the salt-desert zone, largely devoid of vegetation except around active springs and playa margins. In the opposite direction, about 200 m higher in elevation and 4 km to the west, conifer woodlands of Utah juniper (*Juniperus osteosperma*) and singleleaf pinyon (*Pinus monophylla*) emerge, along with an understory of upper-desert shrubs. Higher still, > 2300 m asl, sub-alpine woodlands chiefly of mountain mahogany (*Cercocarpus ledifolius*), Rocky Mountain juniper (*Juniperus scopulorum*), and limber pine (*Pinus flexilis*) mantle the upper slopes of the Goshute Mountains. The nearest perennial sources of water to the rockshelter are both 8 km distant, to the east at Blue Lake marsh along the edge of the salt-desert playa, and to the west at Ferguson Spring in the pinyon-juniper foothills. (For interpretation of the references to colour in this figure legend, the reader is referred to the Web version of this article.)

(Table S2); however, as potentially valid charcoal ages from re-used hearths we still included them in both chronological analyses. Two hearth features from the Stratum 18b/19 (Component VII/VIII) interface (F03.17 and F04.13) contained sagebrush charcoal that dated consistently with other ages from Stratum 18b, but pine (cf. *Pinus flexilis*) charcoal from the same features dated ~1600 calendar years older. Although we suspect that the old pine wood came from organic-rich, otherwise uncharred, deposits (Stratum 19) below the hearths, it is also possible that they represent old pine wood preserved in pre-existing woodrat nests in the shelter that humans collected for use as fuel in these hearths. Such use of old wood could be the cause of discordant charcoal dates in some of the other hearths as well.

Lastly, we note that the age on paleontological bone from below Component VIII (15,235 ± 50 ^{14}C yr BP) was excluded from the chronological analyses because it came from deposits well below the earliest evidence of human occupation of the rockshelter.

2.2. Calibration, Bayesian, and occupation-intensity analyses

The radiocarbon ages from Bonneville Estates were calibrated using the IntCal20 radiocarbon age calibration curve and the OxCal 4.4 radiocarbon calibration program (Bronk Ramsey, 2009; Reimer et al., 2020). Once calibrated, we developed a Bayesian sequence model of 227 stratigraphically consistent radiocarbon ages from components VIII-I. Bayesian models are an effective approach to analyzing large samples of radiocarbon ages, in that they incorporate contextual information in their computations and provide statistically generated calendar ages of not just individual radiocarbon ages relative to their series, but also the starting and ending ages of stratigraphic layers, cultural components, and even cultural complexes in a sequence (e.g., Burley and Edinborough, 2014; Higham et al., 2016). We developed the Bayesian model in OxCal 4.4 by applying the Sequence command for the entire sample, the Boundary command to calculate each component's modeled start and end dates, the Combine command to pool multiple ages from individual features, and the R_Combine command to pool multiple ages from individual specimens (i.e., a single basket or bone). The confidence interval for the analysis was set at 95.4%. In the first run, including all the combined ages, agreement indices indicated poor agreement between unmodeled (prior) and modeled (posterior) calibrated ranges, with A_{model} equaling only 0.5% and $A_{overall}$ equaled 2.0%. This was largely due to poor agreement in the combined ages of nine of the features. The results of this rejected analysis are presented in Table S2. We then decoupled the combined ages that were in poor agreement, re-ran the model, and obtained good overall agreement, with A_{model} equaling 65.4% and

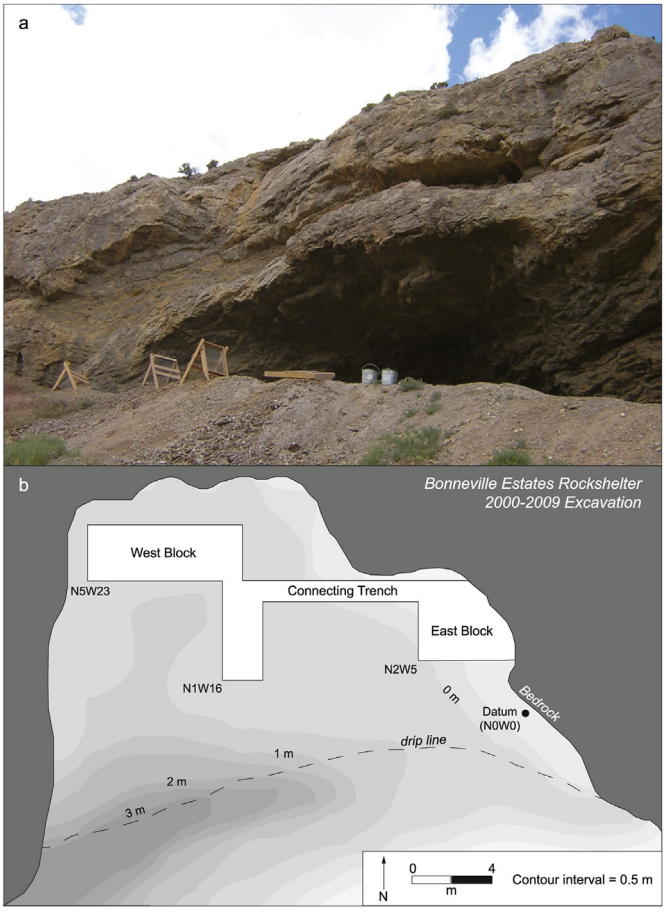

Fig. 4. (a) View of Bonneville Estates Rockshelter; (b) map of excavation, showing surface topography of the rockshelter's interior space. The shelter opens to the southeast and is carved into dolomite bedrock, creating an enclosed space 28 m wide at its front, up to 16 m from front to back, and with a ceiling as much as 10 m above the modern surface. The excavation included the West Block, East Block, and Connecting Trench, as labeled.

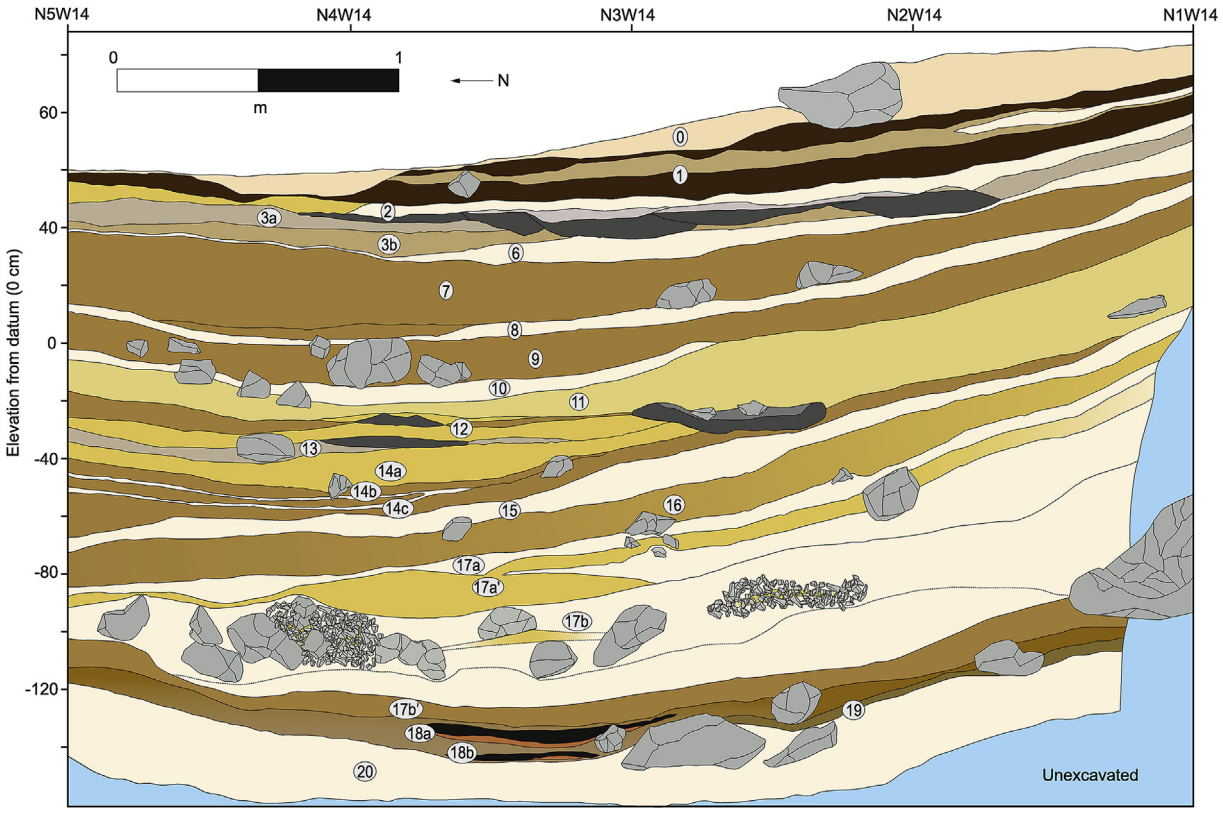

Fig. 5. Representative stratigraphic profile of Bonneville Estates Rockshelter, along the W14 grid line (east wall of the West Block), from north (left) to south (right). Component VII (Dry Gulch Phase) in this area of the excavation was composed of strata 18b–17b'; Component VI (Wendover Phase), strata 17b and 17a'; Component V (Pie Creek Phase), strata 17a-12; Component IV (South Fork Phase), Stratum 11; Component III (James Creek Phase), strata 10-3b; Component II (Maggie Creek Phase), strata 3a-2; Component I (Eagle Rock Phase), Stratum 1. Component VIII was missing from this area of the rockshelter.

$A_{overall}$ equaling 90.1%. Fig. 6(a and b) graphically displays the modeled ages. Probably the poor agreement among the nine hearths relates to re-use of the same hearths.

In a separate analysis we used the KDE_Model command (KDE_Model("site_name", N(01), U(0,1)) in OxCal 4.4 to produce a summed-probability and kernel-density distribution chart of a subset of 245 dates from components VIII-I, again using the Combine and R_Combine commands to pool multiple concordant dates from individual features and specimens, respectively. The KDE_Model command applies the Silverman bandwidth estimate (Bronk Ramsey, 2017) to calculate a kernel-density distribution graphically depicting trends in the distribution of the date series, reducing 'noise' resulting from the radiocarbon-calibration process that can lead to extremes in the summed-probability analysis (Bronk Ramsey, 2017). Our objective in creating these distributions was to measure the probability density of the radiocarbon sample, interpret temporal variability in the intensity of occupation at Bonneville Estates, and consider it in relation to regional environmental proxy records. Our intent was not to extrapolate this single site's record as a reflection of regional demographic trends, which can be problematic (e.g., Surovell and Brantingham, 2007; Bamforth and Grund, 2012; Williams, 2012; Contreras and Meadows, 2014), but to specifically show how significant environmental/climate change could incite variation in human-occupation intensity at a single site in a marginal environmental setting.

3. Results

Unmodelled calendar ages are presented in Table 1. At the 95% confidence interval, the putative Pre-Clovis occupation preserved in Stratum 19 and labeled Component VIII yielded calendar ages from 14,516 ± 182 to 13,397 ± 45 cal yr BP. The more intensive Dry Gulch (Paleoindian) occupation (Component VII) yielded ages from 12,941 ± 71 to 10,531 ± 82 cal yr BP, while the extremely sparse Wendover occupation (Component VI) that followed yielded ages from 10,021 ± 105 to 8581 ± 53 cal yr BP. Dates from the repeated and prolonged Pie Creek occupation (Component V) spanned from 8257 ± 50 to 4792 ± 70 cal yr BP. The relatively brief South Fork occupation (Component IV) yielded ages from 4717 ± 86 to 4156 ± 75 cal yr BP, while the ensuing long James Creek occupation (Component III) dated from 4005 ± 65 to 1418 ± 53 cal yr BP. The uppermost occupations — Maggie Creek (Component II) and Eagle Rock (Component I) — yielded ages ranging from 1405 ± 52 to 856 ± 71 cal yr BP and from 481 ± 50 to 130 ± 76 cal yr BP, respectively.

3.1. Bayesian chronological model

The results of the Bayesian chronological model are presented in Table 1 and Fig. 6(a and b). The most obvious result is that Bonneville Estates' archaeological record was broadly continuous, at least from Clovis times (~13,000 cal yr BP) to latest prehistory (~150 cal yr BP). However, variations in intensity of occupation are evident, and cases can be made for multiple discontinuities reaching 650 years in duration.

Component VIII, the putative 'Pre-Clovis' occupation of the rockshelter, is represented by six modeled dates. Together they indicate a modeled beginning age of 14,574 ± 253 cal yr BP and ending age of 13,256 ± 129 cal yr BP for the component, a span of

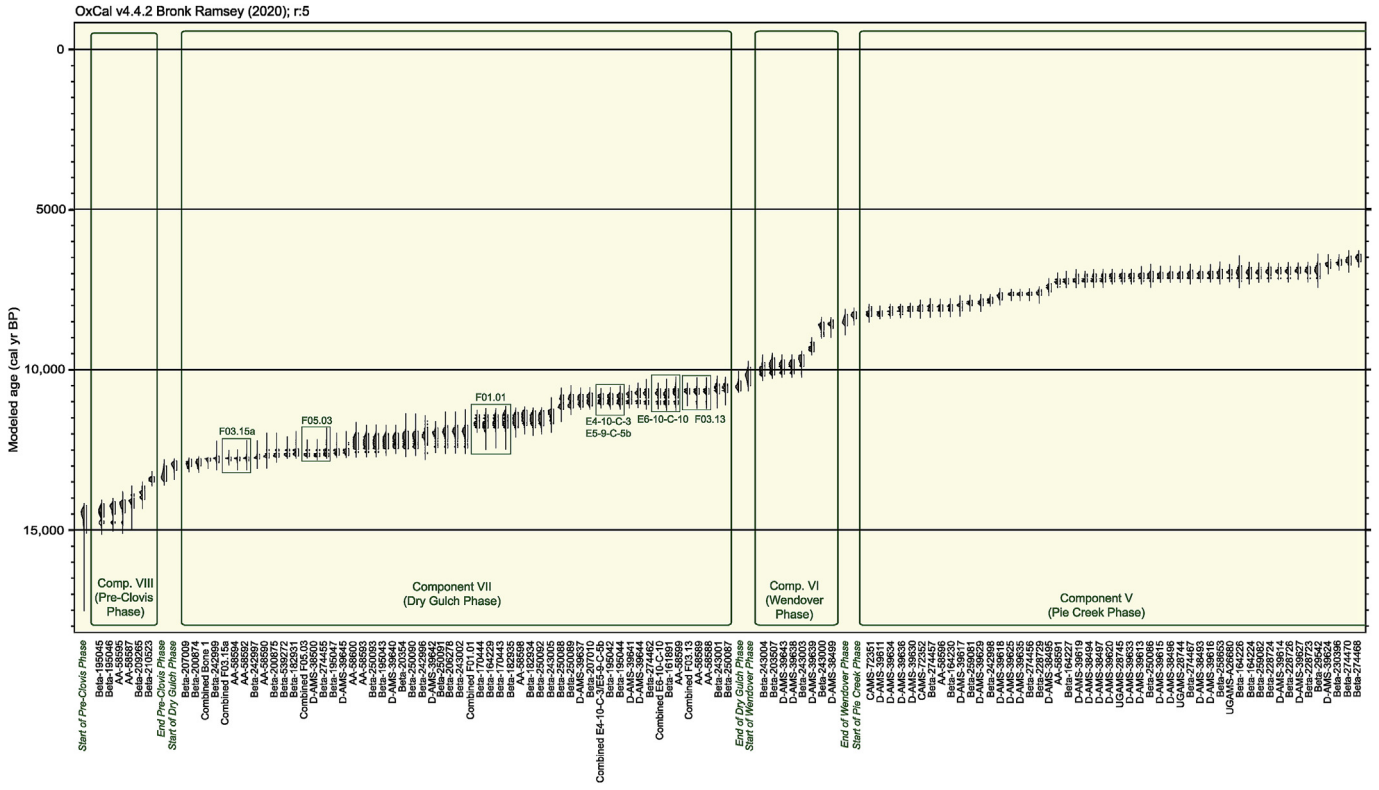

Fig. 6a. Modeled radiocarbon ages (in cal yr BP) for Bonneville Estates Rockshelter, continued in Fig. 6(b), below. Features with multiple radiocarbon ages are grouped in boxes and labeled. Modeled ages for starts and ends of cultural components (phases) are also shown.

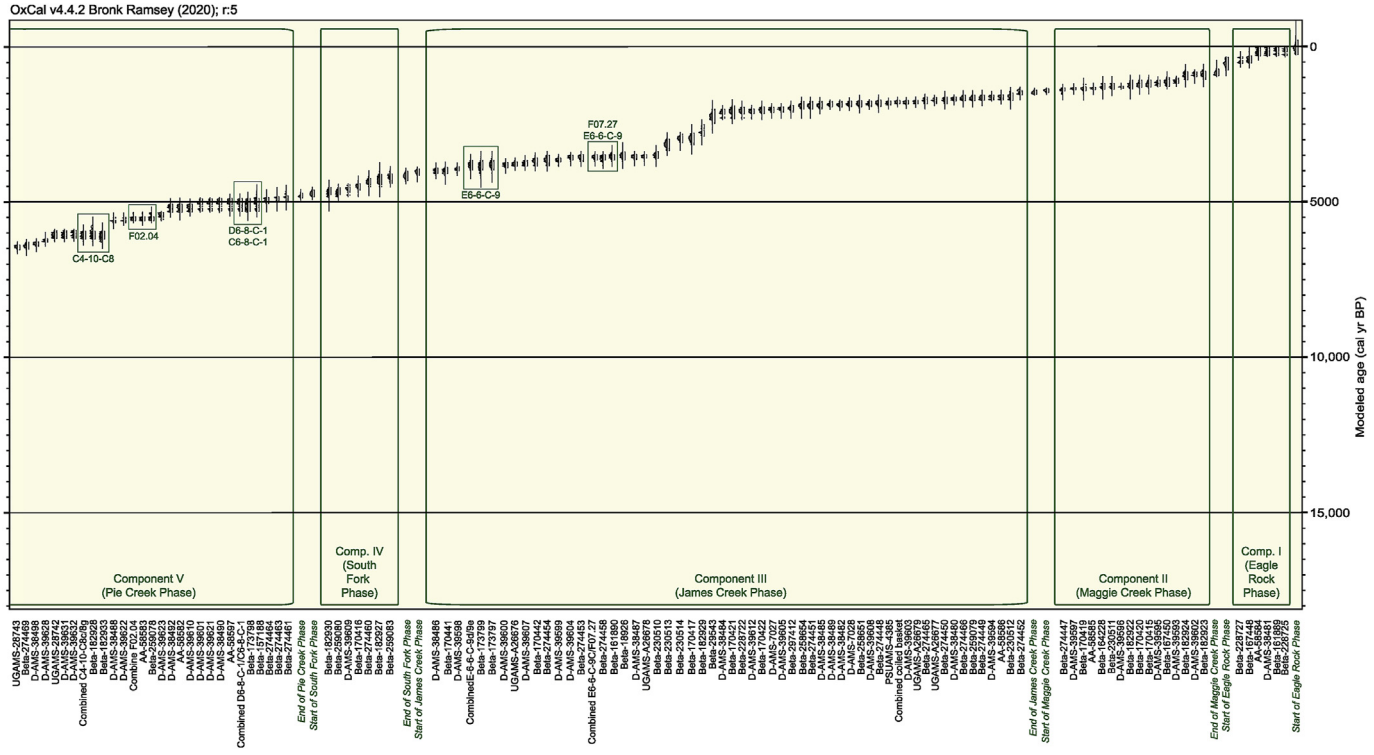

Fig. 6b. Modeled radiocarbon dates (in cal yr BP) for Bonneville Estates Rockshelter, continued from Fig. 6(a) above. Features with multiple radiocarbon ages are grouped in boxes and labeled. Modeled ages for starts and ends of cultural components (phases) are also shown.

Table 1
Unmodeled and modeled calendar ages for Bonneville Estates Rockshelter.

Lab Number	Corrected Radiocarbon Age (1 σ)	Unmodelled Calendar Age				Sequence-modeled Calendar Age				Sequence Model Comments
		Range	μ	2 σ	m	Range	μ	2 σ	M	
End of Eagle Rock Phase	-	–	–	–	–	245–0	16	129	26	Date may extend out of range
Beta-228725	50 ± 40	263–25	130	76	117	266–0	153	83	132	Date may extend out of range
Beta-161889	80 ± 40	268–14	130	77	115	275–24	158	79	137	Date may extend out of range
D-AMS-38481	155 ± 20	284-modern	148	86	164	285–3	176	77	194	Date may extend out of range
AA-58584	160 ± 30	287-modern	150	86	167	289–3	177	77	193	Date may extend out of range
Beta-167448	370 ± 70	523–297	406	71	409	514–292	390	69	381	Date may extend out of range
Beta-228,728[b]	400 ± 40	517–318	435	61	459	–	–	–	–	
Beta-228727	440 ± 40	542–330	481	50	497	533–319	444	71	478	
Beta-297,411[b]	1400 ± 30	1350–1284	1314	21	1310	–	–	–	–	
Start of Eagle Rock Phase	-	–	–	–	–	752–337	537	109	532	
End of Maggie Creek Phase	-	–	–	–	–	934–719	842	59	850	
Beta-182923	960 ± 70	1050–725	856	71	854	1055–791	910	59	911	
D-AMS-39602‡1	985 ± 25	955–795	872	45	863	958–804	900	37	914	
Beta-182924	1010 ± 70	1062–744	905	83	909	1065–800	943	70	939	
D-AMS-39593	1185 ± 20	1178–1009	1106	42	1105	1178–1008	1106	42	1105	
Beta-167450	1210 ± 50	1276–978	1134	72	1131	1275–992	1134	72	1132	
D-AMS-39595	1240 ± 25	1269–1072	1177	55	1162	1269–1072	1177	55	1164	
Beta-170415	1280 ± 60	1299–1067	1197	66	1207	1298–1069	1197	66	1207	
Beta-170420	1300 ± 60	1305–1071	1212	63	1218	1306–1071	1212	62	1218	
Beta-182922	1340 ± 70	1363–1073	1240	69	1249	1359–1074	1239	68	1248	
Beta-230,511‡1	1370 ± 60	1382–1175	1274	59	1287	1375–1175	1272	57	1286	
D-AMS-39596‡2	1370 ± 21	1340–1274	1293	17	1294	1339–1273	1293	16	1294	
Beta-164228	1380 ± 60	1382–1176	1285	58	1296	1373–1176	1283	56	1294	
AA-58585	1415 ± 35	1368–1285	1322	22	1322	1363–1285	1321	21	1321	
Beta-170419	1440 ± 60	1513–1179	1343	51	1338	1403–1194	1328	37	1330	
D-AMS-39597	1455 ± 25	1374–1302	1335	19	1333	1371–1302	1333	18	1332	
Beta-274447	1520 ± 40	1518–1311	1405	52	1393	1408–1307	1361	28	1362	
D-AMS-38479‡1[b]	1735 ± 25	1702–1547	1628	44	1621	–	–	–	–	
Beta-157,189[b]	2220 ± 40	2336–2126	2228	60	2227	–	–	–	–	
Beta-167,449‡2[b]	3350 ± 70	3824–3407	3589	91	3582	–	–	–	–	
Start of Maggie Creek Phase	-	–	–	–	–	1461–1335	1394	31	1391	
End of James Creek Phase	-	–	–	–	–	1520–1383	1458	36	1462	
Beta-274452	1530 ± 40	1521–1317	1418	53	1404	1536–1400	1490	30	1498	
Beta-230512	1690 ± 60	1710–1414	1582	77	1582	1716–1471	1596	66	1590	
AA-58586	1710 ± 35	1700–1533	1609	50	1599	1701–1533	1609	50	1599	
D-AMS-39594	1715 ± 20	1697–1541	1611	47	1599	1697–1541	1611	47	1599	
Beta-274449	1740 ± 40	1710–1544	1631	49	1629	1710–1544	1631	48	1629	
Beta-259079	1760 ± 40	1725–1546	1646	48	1646	1725–1546	1645	48	1645	
Beta-274466	1760 ± 40	1725–1546	1646	48	1646	1725–1547	1646	48	1646	
D-AMS-38480	1783 ± 25	1734–1606	1664	35	1656	1733–1607	1664	35	1656	
Beta-274450	1810 ± 40	1824–1604	1702	59	1708	1824–1605	1702	58	1708	
UGAMS-A26677	1815 ± 25	1817–1623	1707	41	1715	1816–1623	1707	41	1715	
Beta-274465	1820 ± 40	1827–1613	1718	59	1721	1827–1613	1718	59	1721	
UGAMS-A26673‡3a	1850 ± 25	1823–1711	1760	35	1757	–	–	–	–	
UGAMS-A26679	1855 ± 25	1824–1713	1765	34	1765	1824–1713	1765	34	1764	
‡[3a]Combined basket artifact	-	1824–1718	1772	31	1772	1824–1718	1772	31	1771	A = 99.7; C = 99.8
D-AMS-39603	1870 ± 20	1829–1718	1778	32	1778	1829–1718	1778	32	1778	
Beta-274448	1890 ± 40	1920–1712	1800	51	1796	1919–1711	1800	51	1796	
PSUAMS-4385‡[3]	1900 ± 20	1872–1738	1800	37	1799	1872–1738	1800	37	1800	
Beta-164,225‡[3a]	1900 ± 40	1924–1716	1810	54	1806	–	–	–	–	
Beta-258651	1910 ± 40	1927–1725	1821	56	1820	1927–1725	1821	56	1820	
D-AMS-39608	1915 ± 20	1919–1742	1827	43	1832	1918–1742	1827	42	1832	
D-AMS-7028‡[3]	1920 ± 25	1923–1743	1833	46	1837	1923–1742	1833	46	1838	
D-AMS-38489	1930 ± 25	1925–1747	1847	42	1851	1925–1747	1847	41	1851	
D-AMS-38482‡[3]	1935 ± 25	1929–1747	1855	41	1856	1930–1748	1854	41	1856	
UGAMS-A26674[b]	1950 ± 25	1980–1822	1877	37	1876	–	–	–	–	
D-AMS-38485‡4	1955 ± 35	1989–1747	1878	53	1879	1989–1748	1878	53	1879	
Beta-274451	1960 ± 40	1993–1748	1886	56	1887	1993–1748	1886	56	1887	
Beta-258654	1960 ± 40	1993–1748	1886	56	1887	1993–1749	1886	56	1887	
Beta-297412	2030 ± 30	2096–1882	1969	45	1966	2096–1881	1969	44	1967	
D-AMS-39605	2050 ± 25	2100–1927	1996	43	1993	2100–1927	1996	43	1993	
D-AMS-7027	2060 ± 25	2104–1939	2015	45	2016	2104–1940	2015	44	2016	
Beta-170422	2070 ± 40	2146–1925	2032	63	2031	2145–1925	2032	63	2031	
Beta-228722	2090 ± 40	2290–1941	2058	67	2053	2290–1940	2058	67	2053	
Beta-170421	2100 ± 60	2305–1891	2080	98	2069	2305–1892	2080	98	2069	
UGAMS-A26672[b]	2105 ± 25	2143–1995	2064	45	2064	–	–	–	–	
D-AMS-39612‡3	2105 ± 25	2145–1996	2067	48	2066	2144–1995	2067	48	2066	

Table 1 (*continued*)

Lab Number	Corrected Radiocarbon Age (1 σ)	Unmodelled Calendar Age				Sequence-modeled Calendar Age				Sequence Model Comments
		Range	μ	2 σ	m	Range	μ	2 σ	M	
UGAMS-A26675[b]	2120 ± 25	2286–2001	2085	57	2080	–	–	–	–	
D-AMS-38484‡4	2140 ± 30	2299–2000	2126	81	2112	2299–2000	2126	81	2112	
Beta-29543	2250 ± 80	2462–2002	2240	108	2233	2461–2002	2240	108	2234	
Beta-182,929‡5	2620 ± 60	2866–2495	2721	92	2745	2866–2496	2721	92	2745	
Beta-170,417‡5	2820 ± 70	3148–2768	2942	94	2934	3147–2770	2942	94	2935	
Beta-230514	2830 ± 40	3070–2805	2939	60	2935	3070–2801	2939	60	2935	
Beta-230513	2960 ± 60	3336–2956	3125	95	3123	3335–2955	3125	95	3123	
Beta-230510	3260 ± 50	3613–3370	3482	58	3477	3580–3370	3482	58	3477	
UGAMS-A26681[b]	3270 ± 25	3562–3409	3485	36	3477	–	–	–	–	
Beta-161,890‡6	3270 ± 50	3620–3379	3493	59	3488	3636–3466	3545	47	3539	
Beta-182926	3270 ± 60	3636–3373	3497	69	3492	3636–3372	3497	69	3492	
UGAMS-A26678	3305 ± 25	3570–3461	3520	32	3521	3571–3462	3520	32	3521	
D-AMS-38487	3310 ± 30	3618–3453	3524	39	3523	3618–3453	3524	39	3523	
‡6Combined Feature E6-6-C-9C/F07.27	-	3636–3467	3545	47	3539	3636–3466	3545	47	3539	$A_{comb} = 72.2$; C = 99.7
Beta-274453	3330 ± 40	3684–3457	3551	56	3545	3684–3458	3551	56	3545	
D-AMS-39604	3335 ± 25	3635–3481	3543	42	3537	3635–3479	3543	42	3537	
Beta-274,458‡6	3370 ± 40	3700–3481	3602	62	3603	3636–3466	3545	47	3539	
Beta-274,454‡7	3390 ± 50	3822–3484	3631	77	3626	3823–3484	3631	77	3626	
D-AMS-39599	3390 ± 25	3692–3570	3629	40	3625	3692–3570	3629	40	3625	
Beta-170,442‡7	3420 ± 40	3827–3565	3672	70	3664	3827–3565	3672	70	3664	
D-AMS-39607	3470 ± 25	3831–3644	3747	53	3749	3831–3644	3747	53	3749	
UGAMS-A26676	3490 ± 25	3836–3692	3762	44	3761	3837–3691	3762	44	3761	
‡[8]Combined Feature E6-6-C-9d/9e	-	3973–3645	3808	80	3804	3969–3646	3805	77	3802	$A_{comb} = 108.5$; C = 99.5
Beta-173,797‡[8]	3500 ± 70	3970–3575	3772	97	3771	3969–3646	3805	77	3802	
D-AMS-39600	3525 ± 25	3882–3700	3789	48	3783	3882–3715	3789	48	3783	
Beta-173,799‡[8]	3580 ± 90	4149–3637	3883	129	3882	3965–3646	3805	77	3802	
D-AMS-39598	3620 ± 25	3984–3849	3931	38	3928	3982–3850	3926	33	3925	
D-AMS-38486‡[3]	3665 ± 30	4088–3902	4003	56	3999	4070–3893	3963	45	3957	
Beta-170,441‡[7]	3670 ± 40	4145–3886	4005	65	4004	4076–3875	3958	50	3951	
D-AMS-39606[b]	5730 ± 30	6629–6442	6526	50	6524	–	–	–	–	
Beta-274,459[a]	5790 ± 40	6726–6487	6588	55	6590	–	–	–	–	
Beta-182,925[b]	6180 ± 50	7247–6945	7075	73	7073	–	–	–	–	
Start of James Creek Phase	-	–	–	–	–	4134–3929	4024	54	4017	
End of South Fork Phase	-	–	–	–	–	439–4000	4153	76	4152	
Beta-259083	3780 ± 40	4293–3988	4156	75	4154	4402–4091	4223	72	4217	
Beta-182,927‡[9]	3850 ± 70	4506–4002	4261	105	4264	4508–4105	4298	86	4300	
Beta-274460	3910 ± 40	4508–4163	4337	65	4340	4509–4234	4342	62	4346	
Beta-170416	4020 ± 40	4784–4410	4494	66	4484	4612–4411	4489	54	4483	
D-AMS-39609‡[9]	4080 ± 25	4797–4445	4586	88	4564	4781–4444	4562	61	4558	
Beta-259080	4180 ± 40	4838–4580	4714	73	4716	4763–4531	4658	58	4656	
Beta-182930	4200 ± 60	4859–4533	4717	86	4721	4766–4525	4648	65	4650	
Start of South Fork Phase	-	–	–	–	–	4835–4616	4728	57	4731	
End of Pie Creek Phase	-	–	–	–	–	4870–4712	4809	37	4816	
Beta-203505[b]	1560 ± 40	1530–1363	1447	48	1450	–	–	–	–	
Beta-203506[b]	2190 ± 40	2331–2065	2209	71	2216	–	–	–	–	
D-AMS-38491[b]	2940 ± 25	3204–2969	3092	52	3097	–	–	–	–	
D-AMS-39626[b]	3160 ± 25	3449–3347	3392	32	3388	–	–	–	–	
D-AMS-38483‡10[a]	4250 ± 25	4862–4655	4814	50	4835	–	–	–	–	
Beta-274461	4250 ± 40	4951–4624	4792	70	4828	4960–4802	4848	31	4844	
Beta-274463	4300 ± 40	4974–4736	4878	51	4863	4966–4829	4885	45	4866	
Beta-157,188‡11	4320 ± 70	5276–4647	4925	119	4914	5280–4863	5039	118	5012	
Beta-274464	4330 ± 40	5030–4835	4910	52	4904	5030–4836	4911	51	4906	
AA-58597	4410 ± 40	5276–4861	5014	110	4990	5276–4861	5014	110	4991	
D-AMS-38490	4410 ± 35	5270–4865	5005	101	4987	5270–4865	5005	101	4987	
D-AMS-39621	4430 ± 30	5275–4873	5040	107	5013	5275–4873	5040	107	5013	
D-AMS-39601	4430 ± 25	5276–4876	5051	107	5020	5276–4876	5052	107	5019	
‡[11]Combined Feature D6-8-C-1/C6-8-C-1	-	5280–4863	5039	119	5012	5280–4863	5039	118	5012	$A_{comb} = 58.3$; C = 99.5
Beta-173,798‡[11]	4490 ± 60	5315–4885	5138	109	5143	5280–4863	5039	118	5012	
D-AMS-39610	4515 ± 25	5304–5050	5165	77	5156	5303–5050	5165	76	5155	
AA-58582	4530 ± 40	5316–5047	5174	86	5161	5315–5047	5174	86	5162	
D-AMS-38492	4535 ± 30	5315–5051	5176	84	5158	5315–5051	5176	83	5159	
D-AMS-39623	4690 ± 25	5554–5320	5400	56	5388	5553–5320	5400	56	5388	
Beta-259,078‡[12]	4740 ± 40	5583–5326	5472	80	5486	5587–5464	5521	47	5527	
‡[12]Combined Feature 02.04	-	5587–5335	5520	48	5527	5587–5464	5521	47	5527	$A_{comb} = 105.0$; C = 99.6
AA-58583‡[12]	4795 ± 40	5596–5335	5521	51	5522	5587–5464	5521	47	5527	
D-AMS-39622	4850 ± 25	5651–5481	5564	45	5586	5652–5480	5565	45	5586	
D-AMS-38488	4865 ± 30	5658–5485	5596	40	5595	5658–5485	5596	39	5595	
Beta-182,928‡[13]	5160 ± 80	6183–5720	5916	119	5918	6190–5927	6060	80	6061	
‡[13]Combined Feature C4-10-C-8c/8g	-	6190–5927	6060	80	6061	6190–5927	6060	80	6061	$A_{comb} = 63.0$; C = 99.5
D-AMS-39632	5260 ± 25	6178–5935	6049	74	6054	6178–5935	6049	74	6054	
D-AMS-39631	5285 ± 30	6186–5944	6078	65	6080	6186–5944	6078	65	6080	
UGAMS-28742	5300 ± 30	6190–5950	6086	63	6082	6190–5950	6086	63	6082	

(*continued on next page*)

Table 1 (*continued*)

Lab Number	Corrected Radiocarbon Age (1 σ)	Unmodelled Calendar Age				Sequence-modeled Calendar Age				Sequence Model Comments
		Range	μ	2 σ	m	Range	μ	2 σ	M	
Beta-182,933‡[13]	5350 ± 70	6287–5945	6128	92	6130	6190–5927	6060	80	6061	
D-AMS-39628	5460 ± 30	6305–6200	6254	34	6249	6305–6200	6255	34	6251	
D-AMS-38498	5585 ± 30	6437–6300	6357	34	6355	6436–6300	6357	34	6355	
Beta-274,469‡[14]	5650 ± 40	6534–6310	6426	54	6428	6534–6310	6426	54	6428	
UGAMS-28743	5680 ± 30	6555–6396	6458	42	6457	6554–6396	6458	42	6457	
Beta-274470	5720 ± 40	6630–6406	6515	60	6512	6630–6406	6515	60	6512	
Beta-230396	5790 ± 50	6733–6452	6588	65	6589	6732–6453	6588	65	6589	
D-AMS-39624	5848 ± 30	6744–6561	6667	48	6667	6744–6561	6667	47	6667	
Beta-274,468‡[14]	5890 ± 40	6838–6571	6712	49	6710	6836–6571	6711	48	6710	
Beta-29542	6040 ± 80	7158–6678	6902	114	6893	7157–6679	6902	114	6893	
Beta-228723	6050 ± 40	7150–6786	6899	68	6898	7149–6786	6899	67	6898	
D-AMS-39627	6055 ± 30	6991–6795	6903	56	6906	6991–6795	6903	56	6906	
Beta-228726	6070 ± 40	7154–6792	6930	77	6924	7154–6792	6930	76	6924	
D-AMS-39614	6075 ± 25	7150–6801	6932	58	6929	7150–6801	6932	57	6928	
Beta-228724	6080 ± 40	7155–6795	6947	80	6938	7156–6795	6947	80	6938	
Beta-259082	6100 ± 40	7158–6804	6984	84	6969	7158–6805	6984	84	6969	
Beta-164224	6100 ± 50	7158–6801	6984	92	6972	7158–6801	6984	91	6972	
Beta-164226	6100 ± 80	7233–6748	6980	115	6975	7234–6748	6980	115	6974	
UGAMS-A26680	6110 ± 25	7156–6889	6997	74	6977	7157–6889	6996	74	6977	
Beta-258653	6130 ± 50	7164–6884	7027	84	7018	7164–6883	7027	84	7018	
D-AMS-39616	6135 ± 30	7159–6942	7043	70	7030	7159–6941	7043	70	7031	
D-AMS-38493‡[10]	6150 ± 30	7158–6952	7055	64	7053	7158–6952	7055	64	7053	
Beta-274467	6150 ± 40	7164–6909	7052	69	7051	7164–6908	7052	69	7052	
UGAMS-28744	6160 ± 30	7160–6959	7063	59	7062	7160–6960	7063	59	7062	
D-AMS-38496	6165 ± 30	7162–6960	7066	58	7065	7162–6962	7066	58	7065	
D-AMS-39615‡[15]	6170 ± 30	7162–6978	7068	55	7067	7163–6978	7068	55	7067	
Beta-250086	6180 ± 50	7247–6945	7075	73	7073	7247–6945	7075	73	7073	
UGAMS-A26682[b]	6190 ± 26	7166–6992	7078	51	7077	–	–	–	–	
D-AMS-39613	6195 ± 30	7239–6993	7084	56	7080	7239–6992	7084	56	7080	
D-AMS-39633	6210 ± 30	7245–7000	7094	61	7086	7245–6999	7094	61	7087	
UGAMS-28745	6210 ± 30	7246–6999	7098	64	7088	7246–7000	7097	63	7088	
D-AMS-39620	6215 ± 30	7248–7001	7105	67	7092	7248–7001	7104	67	7093	
D-AMS-38497	6245 ± 35	7257–7015	7153	75	7167	7258–7015	7153	75	7167	
D-AMS-38494	6245 ± 35	7256–7020	7161	73	7178	7256–7020	7161	73	7178	
D-AMS-39619	6260 ± 30	7263–7029	7196	53	7212	7263–7028	7196	53	7212	
Beta-164227	6280 ± 40	7308–7025	7201	57	7210	7307–7025	7201	56	7210	
AA-58591	6315 ± 40	7320–7161	7230	51	7228	7320–7161	7230	51	7227	
D-AMS-38495‡[15]	6340 ± 35	7411–7165	7254	54	7262	7411–7165	7254	54	7262	
Beta-228729	6510 ± 50	7560–7318	7411	60	7412	7560–7317	7411	60	7412	
Beta-274456	6750 ± 50	7681–7513	7609	43	7609	7681–7512	7609	42	7610	
D-AMS-39635	6800 ± 30	7683–7583	7637	28	7638	7683–7583	7637	28	7638	
D-AMS-39625	6815 ± 30	7688–7585	7643	28	7643	7688–7585	7643	27	7643	
D-AMS-39618	6815 ± 30	7690–7585	7644	28	7644	7690–7585	7644	28	7644	
Beta-242998	6870 ± 50	7833–7605	7708	56	7704	7832–7605	7708	56	7704	
D-AMS-39629	7005 ± 30	7933–7748	7846	51	7845	7934–7748	7846	51	7845	
Beta-259081	7090 ± 50	8013–7795	7910	52	7912	8013–7795	7910	52	7911	
D-AMS-39617	7095 ± 35	8007–7843	7918	40	7928	8007–7843	7918	40	7928	
Beta-164230	7190 ± 50	8168–7875	8007	60	7996	8168–7875	8007	60	7996	
AA-58596	7240 ± 45	8171–7971	8067	62	8061	8171–7971	8067	62	8061	
Beta-274457	7250 ± 50	8175–7971	8076	61	8080	8175–7971	8075	61	8079	
CAMS-72352	7280 ± 50	8184–7980	8095	56	8098	8184–7981	8094	55	8098	
D-AMS-39630	7325 ± 30	8184–8029	8107	49	8104	8183–8030	8106	47	8104	
D-AMS-39636	7350 ± 30	8300–8027	8129	68	8120	8281–8028	8122	62	8115	
D-AMS-39634	7375 ± 35	8323–8035	8183	84	8186	8309–8034	8164	76	8179	
CAMS-72351	7420 ± 50	8370–8041	8246	70	8255	8335–8038	8212	68	8214	
D-AMS-39611	7425 ± 30	8338–8180	8257	50	8262	8326–8174	8231	48	8224	
Start of Pie Creek Phase	-	–	–	–	–	8413–8192	8297	58	8295	
End of Wendover Phase	-	–	–	–	–	8628–8284	8474	91	8484	
D-AMS-38499	7810 ± 40	8698–8454	8581	53	8580	8719–8464	8595	55	8590	
Beta-243000	7850 ± 50	8979–8486	8669	103	8640	8979–8536	8677	102	8647	
D-AMS-39639	8310 ± 35	9449–9142	9328	75	9341	9447–9142	9328	75	9340	
Beta-243003	8720 ± 60	9905–9541	9711	118	9690	9897–9544	9708	113	9689	
D-AMS-39638	8815 ± 35	10,131-9686	9870	121	9846	10,122-9686	9858	113	9839	
D-AMS-39643	8825 ± 35	10,146-9697	9902	126	9880	10,126-9693	9886	118	9864	
Beta-203507	8830 ± 60	10,176-9678	9910	145	9900	10,160-9630	9889	137	9878	
Beta-243004	8900 ± 50	10,198-9781	10,021	105	10,026	10,186-9776	9991	104	9991	
Start of Wendover Phase	-	–	–	–	–	10,489-9925	10,194	144	10,183	
End of Dry Gulch Phase	-	–	–	–	–	10,649 −10,345	10,507	77	50,516	
Beta-182,932[b]	1000 ± 50	1052–783	887	62	891	–	–	–	–	
Beta-250087	9330 ± 50	10,692 −10,308	10,531	82	10,536	10,705 −10,439	10,589	63	10,583	
Beta-243001	9340 ± 60	10,711 −10,302	10,543	96	10,547	10,740 −10,442	10,603	73	10,604	

Table 1 (*continued*)

Lab Number	Corrected Radiocarbon Age (1 σ)	Unmodelled Calendar Age				Sequence-modeled Calendar Age				Sequence Model Comments
		Range	μ	2 σ	m	Range	μ	2 σ	M	
AA-58588‡[16]	9430 ± 50	11,060 −10,510	10,674	103	10,660	10,752 −10,576	10,664	62	10,664	
‡[16]Combined Feature 03.13	-	10,750 −10,575	10,660	63	10,661	10,752 −10,576	10,664	62	10,664	$A_{comb} = 127.5$; C = 99.3
AA-58589‡[16]	9440 ± 50	11,065 −10,511	10,691	114	10,672	11,070 −10,583	10,800	142	10,749	
‡[17]Combined Feature E6-10-C-10	-	11,070 −10,581	10,798	142	10,748	11,070 −10,583	10,800	142	10,749	$A_{comb} = 102.0$; C = 99.4
AA-58599‡[17]	9440 ± 75	11,074 −10,440	10,724	158	10,689	11,070 −10,583	10,800	142	10,748	
Beta-274462	9490 ± 50	11,072 −10,581	10,807	146	10,757	11,072 −10,582	10,809	145	10,759	
D-AMS-39644	9495 ± 35	11,069 −10,588	10,809	139	10,754	11,069 −10,590	10,810	138	10,754	
Beta-161,891‡[17]	9520 ± 60	11,100 −10,590	10,866	143	10,853	11,070 −10,583	10,800	142	10,749	
D-AMS-39641	9525 ± 35	11,078 −10,683	10,880	128	10,861	11,078 −10,683	10,881	128	10,861	
Beta-195,044‡[18]	9570 ± 40	11,109 −10,720	10,922	112	10,929	11,092 −10,757	10,922	102	10,931	
‡[18]Combined Feature E4-10-C-3/E5-9-C-5b	-	11,092 −10,757	10,922	101	10,930	11,092 −10,757	10,922	102	10,931	$A_{comb} = 112.2$; C = 99.5
Beta-207010	9580 ± 40	11,141 −10,736	10,929	112	10,931	11,141 −10,736	10,929	112	10,931	
Beta-195,042‡[18]	9580 ± 40	11,141 −10,736	10,929	112	10,931	11,092 −10,757	10,922	102	10,931	
D-AMS-39637	9610 ± 35	11,169 −10,772	10,953	114	10,937	11,168 −10,773	10,953	114	10,937	
Beta-250089	9650 ± 60	11,201 −10,773	10,996	130	11,003	11,201 −10,773	10,996	130	11,002	
Beta-250088	9700 ± 60	11,239 −10,793	11,061	131	11,113	11,239 −10,791	11,061	131	11,114	
Beta-243005	9940 ± 60	11,689 −11,234	11,409	124	11,378	11,689 −11,234	11,409	124	11,377	
AA-58598‡[19]	9995 ± 55	11,730 −11,266	11,485	128	11,477	11,734 −11,265	11,486	128	11,478	
Beta-250092	10,020 ± 50	11,744 −11,280	11,521	124	11,519	11,744 −11,280	11,520	124	11,519	
Beta-182934	10,030 ± 50	11,805 −11,311	11,535	124	11,534	11,806 −11,288	11,535	124	11,534	
Beta-170,443‡[20]	10,040 ± 70	11,815 −11,279	11,554	145	11,552	11,817 −11,403	11,644	108	11,663	
Beta-182,935‡[19]	10,050 ± 50	11,813 −11,330	11,566	126	11,564	11,871 −11,650	11,778	51	11,775	
‡[20]Combined Feature 01.01	-	11,817 −11,403	11,664	108	11,663	11,817 −11,403	11,644	108	11,663	$A_{comb} = 109.0$; C = 99.4
Beta-164,229‡[20]	10,080 ± 50	11,825 −11,352	11,616	130	11,632	11,817 −11,403	11,644	108	11,663	
Beta-170,444‡[20]	10,130 ± 60	11,940 −11,402	11,709	142	11,732	11,817 −11,403	11,644	108	11,663	
Beta-242996	10,200 ± 60	12,428 −11,411	11,870	141	11,868	12,428 −11,413	11,870	140	11,867	
Beta-243002	10,250 ± 60	12,453 −11,748	12,004	174	11,963	12,454 −11,748	12,003	174	11,963	
Beta-206278	10,250 ± 50	12,442 −11,752	11,982	150	11,950	12,441 −11,752	11,982	149	11,949	
Beta-250091	10,260 ± 50	12,447 −11,761	12,012	159	11,973	12,446 −11,760	12,011	159	11,972	
D-AMS-39642	10,285 ± 35	12,443 −11,829	12,057	148	12,014	12,422 −11,830	12,057	148	12,014	
Beta-250090	10,330 ± 50	12,470 −11,937	12,183	162	12,158	12,470 −11,938	12,183	162	12,157	
Beta-203504	10,340 ± 60	12,478 −11,935	12,198	166	12,183	12,478 −11,935	12,199	165	12,183	
D-AMS-39640	10,360 ± 35	12,470 −11,997	12,231	141	12,229	12,469 −11,997	12,231	141	12,229	
Beta-195043	10,380 ± 40	12,477 −12,004	12,256	136	12,256	12,477 −12,005	12,256	135	12,257	
AA-58600‡[19]	10,385 ± 55	12,583 −11,975	12,258	151	12,257	12,583 −11,975	12,258	151	12,258	
Beta-250093	10,400 ± 50	12,587 −12,004	12,278	145	12,277	12,587 −12,003	12,278	145	12,277	
AA-58593	10,405 ± 50		12,285	146	12,283		12,285	146	12,283	

(*continued on next page*)

Table 1 (*continued*)

Lab Number	Corrected Radiocarbon Age (1 σ)	Unmodelled Calendar Age				Sequence-modeled Calendar Age				Sequence Model Comments
		Range	μ	2 σ	m	Range	μ	2 σ	M	
		12,591 −12,004				12,591 −12,005				
D-AMS-39645	10,520 ± 40	12,681 −12,283	12,548	81	12,551	12,681 −12,284	12,549	80	12,551	
Beta-195047	10,540 ± 40	12,677 −12,480	12,567	67	12,562	12,677 −12,480	12,568	67	12,563	
Beta-274,455‡[21]	10,540 ± 60	12,717 −12,197	12,550	110	12,563	12,714 −12,497	12,636	57	12,649	
‡[21]Combined Feature 05.03	-	12,715 −12,496	12,636	57	12,649	12,714 −12,497	12,636	57	12,649	$A_{comb} = 82.9$; C = 99.6
Beta-182931	10,560 ± 50	12,697 −12,480	12,583	76	12,599	12,698 −12,480	12,584	75	12,599	
Beta-539272	10,600 ± 40	12,716 −12,492	12,625	64	12,643	12,716 −12,492	12,625	63	12,643	
Beta-200875	10,640 ± 60	12,737 −12,492	12,647	66	12,664	12,737 −12,492	12,647	66	12,664	
D-AMS-38500‡[21]	10,645 ± 45	12,732 −12,505	12,665	52	12,679	12,714 −12,497	12,636	57	12,649	
AA-58590	10,690 ± 70	12,757 −12,497	12,677	61	12,693	12,757 −12,497	12,677	61	12,693	
Beta-242997	10,720 ± 60	12,760 −12,620	12,705	42	12,714	12,760 −12,620	12,705	42	12,714	
AA-58592‡[22]	10,760 ± 70	12,834 −12,621	12,732	49	12,733	12,821 −12,701	12,742	20	12,741	
Beta-242999	10,790 ± 70	12,888 −12,673	12,757	49	12,748	12,821 −12,701	12,742	20	12,741	
‡[22]Combined Feature 03.15a	-	12,820 −12,701	12,742	20	12,741	12,821 −12,701	12,742	20	12,741	$A_{comb} = 153.4$; C = 99.8
AA-58594‡[22]	10,800 ± 60	12,840 −12,690	12,760	39	12,750	12,821 −12,701	12,742	20	12,741	
Beta-210,524‡[23]	10,830 ± 40	12,827 −12728	12,768	29	12,757	–	–	–	–	
‡[23]Combined bone	-	12,832 −12,741	12,783	28	12,779	12,831 −12,741	12,783	28	12,778	A = 99.7; C = 99.8
UCIAMS-22176‡[23]	10,900 ± 45	12,898 −12,745	12,812	45	12,806	–	–	–	–	
Beta-200874	10,970 ± 60	13,066 −12,760	12,897	83	12,886	12,974 −12,752	12,852	60	12,848	
Beta-207009	11,010 ± 40	13,076 −12,831	12,941	71	12,937	12,995 −12,765	12,884	55	12,876	
Start of Dry Gulch Phase						13,120 −12,821	12,953	77	12,941	
End of Pre-Clovis Phase						13,460 −12,982	13,256	129	13,281	
Beta-210523	11,530 ± 40	13,476 −13,314	13,397	45	13,397	13,488 −13,320	13,409	46	13,412	
Beta-209265	11,960 ± 60	14,035 −13,612	13,866	102	13,860	14,036 −13,612	13,866	102	13,860	
AA-58587	12,180 ± 60	14,318 −13,816	14,098	126	14,088	14,311 −13,861	14,089	102	14,087	
AA-58595	12,270 ± 60	14,808 −14,050	14,276	198	14,214	14,456 −14,045	14,216	122	14,193	
Beta-195046	12,330 ± 40	14,816 −14,108	14,387	211	14,308	14,771 −14,099	14,289	130	14,259	
Beta-195045	12,390 ± 40	14,846 −14,209	14,516	182	14,475	14,785 −14,165	14,381	131	14,361	
Start of Pre-Clovis Phase	-	–	–	–	–	15,085 −14,217	14,574	253	14,511	
Pre-Archaeology										
UCIAMS-22180[a]	15,235 ± 50	18,707-18,283	18,476	124	18,445	–	–	–	–	

‡Included in Bayesian model, but as combined date for feature, artifact, or bone (superscript number links combined ages to pooled age).
[a] Excluded from all radiocarbon analyses.
[b] Excluded from Bayesian model (Fig. 6) but included in the summed-probability/kernel-density analysis (Fig. 7).

~1300 calendar years.

Component VII, the Dry Gulch Phase, is modeled to have begun 12,953 ± 77 cal yr BP and ended 10,507 ± 77 cal yr BP. During this prolonged span of ~2500 calendar years, human activity in the rockshelter was regular and repeated. In the sequence of 56 modeled ages there is only a minor interruption ~11,200 cal yr BP.

During the ensuing Component VI (Wendover Phase) occupation, from 10,194 ± 144 to 8474 ± 91 cal yr BP, a span of ~1700 calendar years, human activity became sporadic and sparse. Only eight modeled ages chronicle the near lack of activity during this period, which is instead characterized as containing among the rockshelter's three longest lulls in human occupation — discontinuities of ~310 calendar years at its start as well as ~350 and ~650 calendar years during its middle.

With the onset of the Component V Pie Creek occupation at 8297 ± 58 cal yr BP, human use of Bonneville Estates intensified significantly. Eighty-one modeled ages chronicle this phase, which did not end until 4809 ± 37 cal yr BP, a span of ~3490 calendar years. During these three-and-a-half millennia, humans frequently visited the rockshelter, and the Bayesian model predicts only one prolonged break in activity, an interval of ~460 calendar years between ~6060 and ~5600 cal yr BP, although five other shorter breaks of ~200 years can be identified, the most prominent ~7500 cal yr BP.

Human occupation continued uninterrupted into both Component IV (South Fork Phase) and Component III (James Creek Phase), indicating that the component transitions are not based on a chronological discontinuity (but instead on detected changes in stratigraphy and material culture, as discussed below). Component IV's South Fork occupation is represented by seven modeled ages as well as start and end times of 4728 ± 57 and 4153 ± 76 cal yr BP, respectively, a brief span of ~575 calendar years. Component III's James Creek occupation, however, is represented by 58 modeled ages, and it has a modeled start at 4024 ± 54 cal yr BP and end at 1458 ± 36 cal yr BP, a span of ~2570 calendar years. Within Component III, there is one obvious discontinuity in the chronology; it is modeled to have persisted for ~580 calendar years from ~2815 to ~2230 cal yr BP. As such, it is the most significant gap in the radiocarbon model after 5000 cal yr BP, and the second-longest in the entire record, after the ~650-year hiatus during the early Holocene. This is followed by a single date of ~2230 cal yr BP and then another shorter gap until ~2070 cal yr BP (~160 years). This span of ~745 years, with only one recorded occupation event, breaks the James Creek phase into clear early and late sub-phases.

There is no obvious gap between the end of Component III and start of Component II, the shift from the James Creek Phase to Maggie Creek Phase (instead the transition is stratigraphic and documented by change in material culture, as discussed below). The model predicts that Component II began 1394 ± 31 cal yr BP and ended 842 ± 59 cal yr BP, a span of ~550 calendar years. The 16 modeled ages for Component II are continuous until the end of the phase.

The transition to Component I (the Eagle Rock Phase) is marked by a discontinuity of ~310 years. Its beginning is modeled at 537 ± 109 cal yr BP, and its end, at 16 ± 129 cal yr BP, with the model warning that the five youngest ages from the component may extend out of range (i.e., beyond 1950 CE). Nonetheless, the component's seven modeled ages suggest a span of ~500 calendar years, indicating that human occupation during the Eagle Rock Phase continued into historic times.

3.2. Summed-probability and kernel-density analysis

The results of the summed-probability/kernel-density analysis are presented in Fig. 7, with component/phase boundaries superimposed (from data presented in Table 1). This analysis provides a second perspective on Bonneville Estates' chronological sequence, complementary to the Bayesian model presented above. The Component VIII putative 'Pre-Clovis' occupation spans from ~14,800 to 13,200 cal yr BP. As recorded in Component VII, intensive Paleoindian (Dry Gulch Phase) use of the rockshelter began ~13,000 cal yr BP, peaked sharply 12,700 cal yr BP, and persisted until 10,400 cal yr BP, with a possible minor lull ~ 11,200 cal yr BP. The successive Wendover Phase of Component VI, persisting for ~2000 calendar years, was a period of infrequent and ephemeral use, with an obvious discontinuity in the record centered around 9000 cal yr BP. Shorter discontinuities occur at the beginning (~10,250 cal yr BP) and possibly at the end (8400 cal yr BP) of Component VI. The second major pulse of human use of the rockshelter is represented by Component V and the onset of the Pie Creek Phase around 8350 cal yr BP. For the next 3500 calendar years, early Archaic humans repeatedly utilized the rockshelter, albeit more intensively during certain episodes than others (i.e., ~8200–7900, 7350–6800, and 6650–6400, 5500, and 5100-4800 cal yr BP). As the Bayesian model suggests, the only prolonged period of sparse human activity during the Pie Creek Phase occurred from 5950 to 5550 cal yr BP. During South Fork times, as represented by Component IV, human activity continued in the rockshelter at a low but relatively continuous pace (from ~4800 to 4050 cal yr BP), and during James Creek times of Component III, there were two pulses of activity ~3800–3400 and 2300-1600 cal yr BP. These were interdigitated by intervals when humans appear to have visited Bonneville Estates infrequently, generally ~3300 to 2350 cal yr BP. After this, the rockshelter saw continued occupation into the Maggie Creek Phase (Component II), with a major spike at 1400 cal yr BP followed by a gradual decline in activity leading up to a ~150-year lull in occupation corresponding to the transition to the Eagle Rock Phase (Component I). Activity during the Eagle Rock Phase (Component I) continued sporadically until historic times.

4. Discussion

4.1. The record of human occupation at Bonneville Estates Rockshelter

Together, the Bayesian sequence model and summed-probability/kernel-density analysis offer complementary accounts of Bonneville Estates Rockshelter's cultural chronology. The Bayesian analysis provides a series of boundary ages for the cultural components, calculating their potential durations as well as possible discontinuities in the record. This is expressed in the changing slope of the line created by the series of dates in the Bayesian sequence model (Fig. 6): a more horizontal slope indicates a time of intensive, regular use of the rockshelter, while a more vertical slope indicates a period of sparse, irregular use. Likewise, the summed-probability/kernel-density analysis (Fig. 7) presents a compilation of the likelihood of human occupation in the rockshelter at any given point in time, so that the resulting curve can be useful for identifying episodes when humans repeatedly and intensively used Bonneville Estates versus when use was infrequent and insignificant. Obviously, the radiocarbon record demonstrates that human occupation of the rockshelter was far from uniform; instead, the rate of occupancy was quite variable and there are even several discontinuities in the record, between and within cultural components. The discussion that follows considers both the Bayesian sequence and summed-probability/kernel-density analysis to create a chronicle of paleoecological and archaeological events, starting with the lowest stratigraphic context to yield a radiocarbon age (the base of Stratum 19; below Component VIII) and progressing upward through the sequence to latest prehistoric times (Stratum 1; Component I).

The most ancient unmodeled radiocarbon age obtained from the Bonneville Estates excavation is 18,476 ± 124 cal yr BP (UCIAMS-22180), on an unidentifiable long-bone fragment of mammal bone from the base of Stratum 19, just above its contact with Stratum 20, in the westernmost area of the West Block. This unmodified bone was not associated with any evidence of human occupation. It correlates with the time that Lake Bonneville catastrophically fell from the Bonneville shoreline (upon which Bonneville Estates is situated) to the Provo shoreline, as it cut through Red Rock Pass near the Utah-Idaho border, an event independently dated to 18,400–17,100 cal yr BP (Oviatt, 2015; Oviatt and Jewell, 2016; Oviatt and Shroder, 2016). This event left the rockshelter 'high and

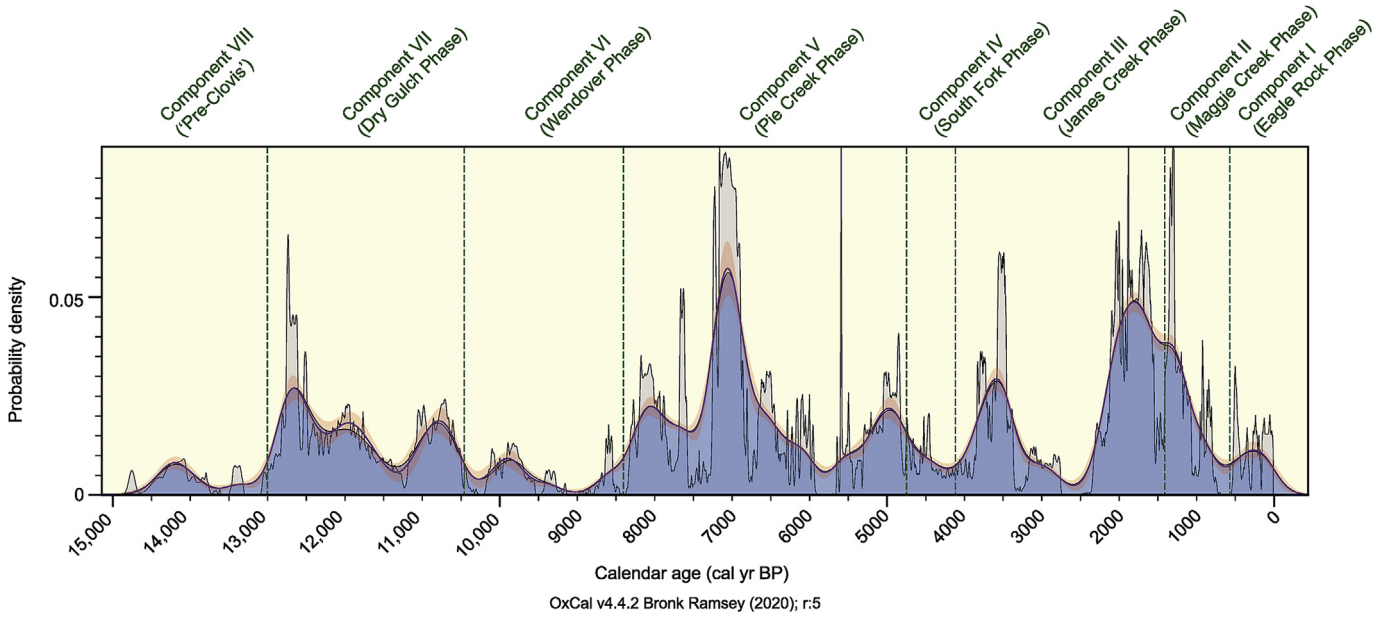

Fig. 7. Summed-probability (sawtoothed line, shaded gray area) and kernel-density (smoothed line with shaded blue area representing means and red band representing 1-σ uncertainty) distributions of radiocarbon ages in the Bonneville Estates Rockshelter sequence. (For interpretation of the references to colour in this figure legend, the reader is referred to the Web version of this article.)

dry' and evidently immediately available for animal and human use. That the date on the bone is so early in the age range of the recession supports interpretations that the initial drop from the Bonneville shoreline occurred very rapidly and relatively early in the accepted age range for this event (Gilbert, 1890; Oviatt, 2015; Oviatt and Jewell, 2016), but it is at odds with most recent interpretations that the Bonneville flood occurred closer to 17,500 ± 500 cal yr BP (Oviatt, 2020).

Stratum 19 in the West Block contains a possible 'Pre-Clovis-aged' occupation, tentatively called Component VIII. Six modeled radiocarbon ages span from 14,381 ± 131 to 13,409 ± 46 cal yr BP; four are on charred plant macrofossils and range from ~14,380 to ~14,090 cal yr BP, while two are on bone and are considerably younger, ~13,870 and ~13,410 cal yr BP (Table 1). Taken together they indicate that Component VIII spanned from about 14,575 to 13,250 cal yr BP. The charred plant samples included vitrified pine charcoal that came from burnt features situated directly underneath and in stratigraphic contact with above-lying Stratum 18b hearths, so likely they are the result of unintentional burning of older, naturally-accumulated organics by Paleoindians who used the rockshelter later in time (Graf, 2007). Alternatively, perhaps the pine charcoal came from fuel use of old wood preserved in woodrat nests, as suggested above. Moreover, only tiny retouching flakes were recovered from Component VIII, mostly under high-density concentrations of flakes in above-lying Component VII; they likely represent down-drift from the immediately overlying deposit.

From the contact of Stratum 19 (Component VIII) with overlying Stratum 18b (the basal deposit of Component VII in the West Block), a small bone fragment yielded a pair of unmodeled ages (12,812 ± 45 [UCIAMS-22176] and 12,768 ± 29 [Beta-210,524] cal yr BP) which when combined yielded a modeled age of 12,783 ± 28 cal yr BP, while charcoal from a nearby hearth feature yielded a modeled age of 12,852 ± 60 (Beta-200894) cal yr BP. These modeled ages help define the lower limit for Stratum 18b in the western area of the West Block where it was best-preserved, ~12,850–12,800 cal yr BP. The modeled beginning age for Component VII, however, is 12,953 ± 77 cal yr BP, due to an older hearth farther east in the excavation. All human occupation of the rockshelter likely post-dates this.

Component VII represents the rockshelter's Paleoindian occupation, locally referred to as the Dry Gulch Phase and regionally as the Western Stemmed Tradition. In the West Block we could easily differentiate between three successive strata rich in organics (substrata 18b, 18a, and 17b′), but in the central area of the excavation these were replaced by a facies of massive sandy loam with small-sized *éboulis* and few organics (Graf, 2007). In the East Block, *éboulis* were larger and organics even rarer; nonetheless, based on variably-sized angular-rock fragments we distinguished two strata, in the field labeling these East Block Stratum 12 and Stratum 10, which we later directly traced through the trench to Stratum 18 and Stratum 17b′ in the main excavation, respectively. Across the entire excavation of Component VII, 56 modeled radiocarbon dates on wood charcoal and charred organics from 41 different hearths provide chronological control over this occupation. These modeled ages range from 12,884 ± 55 (Beta-207009) to 10,589 ± 63 (Beta-250,087) cal yr BP and indicate three pulses of Paleoindian activity, each associated with one of the three Component VII sub-strata: ~12,950–12,550 cal yr BP, 12,300–11,400 cal yr BP, and 11,100–10,600 cal yr BP. Significantly, though, the Bayesian sequence and kernel-density models did not identify perceptible discontinuities in occupation between these sub-strata. The shelter's four earliest hearths predate 12,750 cal yr BP and hence are Clovis-aged (Waters et al., 2020); however, no signs of bifacial-fluting technology were found around these hearths. Instead, diagnostic bifaces from Component VII are stemmed lanceolate points (i.e., Haskett, Parman, Windust varieties) or their preforms (Fig. 2; Goebel 2007; Goebel et al., 2011; Hockett and Goebel, 2019). The end of Component VII at ~10,500 cal yr BP marks the latest time Western Stemmed points occur in the rockshelter's record.

During the time of Component VI, the Wendover Phase, human occupation was sparse, especially compared to the components immediately preceding and succeeding it. Stratigraphically, Component VI is represented by Stratum 17b, a loam zone with

large *éboulis*, which across the rockshelter was mostly devoid of cultural remains (except a few isolated hearths and scarce associated cultural debris). Human occupants left behind no diagnostic bifacial points. Eight modeled ages from four Component VI hearths range from 9991 ± 104 to 8595 ± 55 cal yr BP, leading to a modeled time span of ~10,200–8470 cal yr BP, the great majority of it lacking any dated evidence of occupation. Humans rarely visited Bonneville Estates during the early-mid Holocene, and when they did, their stays were short and their activities limited.

The geochronological character of Component V, assigned to the early Archaic Pie Creek Phase, differs markedly from Component VI. Earliest Component V is represented by Stratum 17a, an ephemeral occupation with two hearths situated at the very top of the Stratum 17 zone of loam and rubble, and then Stratum 16, an organic-rich deposit found across most of the rockshelter's excavation. Stratum 16 was sealed by a culturally sterile deposit of silt and *éboulis*, called Stratum 15. Within Stratum 15, excavations occasionally exposed isolated pockets of a tephra geochemically attributed to the Mt. Mazama eruption in central Oregon (analysis by S. Kuehn; Table S3), independently well-dated to ~7600 cal yr BP (e.g., Zdanowicz et al., 1999; Egan et al., 2015). This conforms well with its position within the radiocarbon chronology, as the youngest modeled age for underlying Stratum 16 is ~7610 cal yr BP and the oldest age for overlying Stratum 14 is ~7410 cal yr BP. Above Stratum 15 is the most intensive occupational period of the middle Holocene, Stratum 14, a widespread organic-rich deposit from which we encountered the most hearths of any Archaic-aged stratum. In the East Block and connecting trench, Component V continues into Stratum 13, which contains another well-preserved cultural occupation. In the West Block, Component V continues into the zone of sandy loam and rubble labeled Stratum 12, mostly devoid of human remains but still containing a pair of dated hearths and a small assemblage of cultural materials. Despite the multiple sandy-loam-and-rubble zones within Component V, its modeled chronology is relatively continuous, indicating a nearly 3500-year-long interval of human use of the rockshelter. The obvious exception is a 460-year discontinuity centered around 5800 cal yr BP, which is associated stratigraphically with the end of Stratum 14 and start of Stratum 13 and represents the culmination of a long period of declining feature construction and use of the shelter. The Bayesian sequence model, moreover, suggests an additional earlier episode of relatively infrequent use around 7500 cal yr BP, associated with the deposition of Stratum 15, which yielded few cultural remains and no hearths. In the Bayesian sequence model, this is noticeable as the relatively steep slope early in the Component V distribution shown in Fig. 6. Despite the periodic breaches or near-breaches in Component V's chronology, however, its entire sequence of 81 modeled ages is characterized by large side-notched bifacial points (Hockett and Goebel, 2019) and ground-stone technology, the defining cultural characteristics of this component. Leppy Hills corner-notched points and Pinto points also occur in the component (Fig. 2).

Component IV, assigned to the South Fork Phase, consists of just one stratigraphic layer, Stratum 11, an organic-rich deposit sandwiched between two deposits of sandy loam and rubble, strata 12 and 10. Its seven modeled radiocarbon ages indicate a steady yet moderately low-in-intensity occupation from ~4700 to 4150 cal yr BP. Although stratigraphically intact with clear lower and upper contacts, Component IV's small bifacial-point assemblage contains a diversity of forms, including Dead Cedar corner-notched, large side-notched, Humboldt, and Elko corner-notched varieties (Hockett and Goebel, 2019). We interpret the component to represent a transitional period in regional prehistory, between the early and middle Archaic.

Like components VII and V, Component III represents a major period of human occupation of Bonneville Estates Rockshelter, the James Creek Phase of the middle Archaic. Stratigraphically it is represented by strata 10 through 3b, with most cultural activity being found in strata 9, 7, and 3b, although a substantial pit feature from the middle of the shelter was attributed also to Stratum 4. Strata 10, 8, and 6 represent silty deposits with variable amounts of *éboulis*. Hence, like Component V, the stratigraphic sequence for Component III suggests episodic occupation zones separated by deposition of layers of mostly sandy loam and rubble with few cultural remains. The modeled radiocarbon chronology of 58 ages follows this stratigraphic characterization with two major pulses of activity centered at 3600 (Stratum 9) and 1850 (strata 7, 4, and 3b) cal yr BP, as well as in between a prolonged 580-year discontinuity centered around 2500 cal yr BP (the silt deposit of Stratum 8). Bifacial points throughout Component III are predominantly of the Elko corner-notched series (Fig. 2), expectable for the late-middle Archaic James Creek Phase; however, early Component III also yielded large side-notched, Humboldt, Gatecliff, and Dead Cedar corner-notched points, while late Component III contains a few Rosegate corner-notched and variable side-notched points in its uppermost portion (Hockett and Goebel, 2019).

Component II represents an interval of intensive human occupation. Across the rockshelter, this period is represented by upper Stratum 3, an organic-rich zone with numerous hearth features and pit features ascribed to the Maggie Creek Phase of the late Archaic. Sixteen modeled radiocarbon ages indicate a uniform and unbroken sequence from around 1390 to 840 cal yr BP, and the summed-probability/kernel-density analysis demonstrates a strong peak in occupation ~1350 cal yr BP. There are no signs of a temporal gap between components III and II, significant in that this transition correlates to the appearance of bow-and-arrow technology at the rockshelter, in the form of Rosegate series points (Fig. 2; Hockett and Goebel, 2019). The modeled age span of the Maggie Creek Phase overlaps with the time of the Fremont culture of the eastern Great Basin and northern Colorado Plateau, and not surprisingly, a few material-culture signs of the Fremont occur in Component II's assemblage: sherds of undecorated grayware pottery and a few kernels of maize, the latter with a direct modeled age of 900 ± 37 cal yr BP (D-AMS-39602). Whether these occupants were Fremont, or only knew of Fremont people across the Bonneville basin to the south and east, clearly they visited Bonneville Estates Rockshelter regularly and created a strong archaeological record of their activities.

The final phase of cultural occupation at Bonneville Estates is represented by Component I, the Eagle Rock Phase of the late Archaic. Its cultural remains are found straddling the strata 2–1 contact, the late-prehistoric surface later mantled by domesticated-sheep (*Ovis aries*) dung of the historic period. Component I's modeled span of seven ages began ~530 cal yr BP, after a modeled discontinuity of ~150 years associated with the Component II/Component I transition. Bifacial points from Component I are quite variable but include typical late Archaic forms including Rosegate series points, Cottonwood triangular points, and small side-notched points (Fig. 2; Hockett and Goebel, 2019). The recovery of single Clovis, Humboldt, and Gatecliff points from Component I indicates either late-prehistoric borrowing and re-use or some mixing of the historic surface with earlier sediment and artifacts through modern looting.

4.2. Interpreting the effects of climate

In a general sense, our construction of a thorough radiocarbon chronology dating nearly all archaeological hearths as well as other

features encountered in our excavations indicates that Bonneville Estates Rockshelter contains a sustained record of human activity beginning by about 13,000 cal yr BP. Paleoindians of the Dry Gulch Phase repeatedly inhabited the rockshelter, as did early Archaic foragers of the Pie Creek Phase and middle Archaic foragers of the South Fork and James Creek phases. Human occupation continued unabated during the relatively brief Maggie Creek Phase of the late Archaic, and despite the presence of three older point forms in Component I, the multiple hearth features and arrow points of the Eagle Rock Phase indicate continued regular human occupation leading up to the historic period.

Under closer scrutiny, however, we clearly see that the *tempo* of occupation was far from uniform. In the Bayesian sequence analysis, discontinuities in the radiocarbon chronology were documented by a series of small vertical jumps in the slope of an otherwise gradually upward-through-time trajectory of modeled radiocarbon dates (Fig. 6); and in the summed-probability/kernel-density analysis, probability densities repeatedly rose and fell, with as many as ten discernible peaks and nine intervening valleys (Fig. 7). The most significant of the peaks are centered around 12,600, 8000, 7000, 4800, 3600, 1800, and 1300 cal yr BP, while significant valleys occur around 10,300, 9000, 5800, 4200, 2600, and 600 cal yr BP. We hypothesize that the variable tempo in site visits, accentuated by the modeled gaps in the record, are the product of climate-induced change in environmental conditions affecting local hunter-gatherer subsistence and settlement behavior.

To test the hypothesis, we consulted a growing body of paleoenvironmental records for the eastern and central Great Basin, coupled with additional data from the western Great Basin and Sierra Nevada mountains of western Nevada and eastern California (Fig. 8; locations of important paleoecological sites are shown in Fig. 1). A summary of paleoenvironmental change and potential correlation with the Bonneville Estates record is presented below.

4.2.1. Latest Pleistocene (~13,000–11,700 cal yr BP)

Following the creation of a huge, deep freshwater Bonneville lake (Oviatt, 2015), significant warming and drying led to the lake's rapid regression and partial desiccation during the Bølling-Allerød interstadial, starting around 14,800 cal yr BP and reaching modern Great Salt Lake levels by 13,000 cal yr BP (Reheis, 2014; Spencer et al., 2015; Broughton and Smith, 2016). This is coincident with the deposition of strata 20 and 19 in Bonneville Estates Rockshelter, presumably non-cultural (Component VIII) sediments predating 13,250 cal yr BP. Woodrat middens dating prior to 12,800 cal yr BP show that the vicinity of the rockshelter supported a mosaic of sagebrush-dominated shrubland and limber-pine woodland (Rhode, 2016).

Sometime after 13,000 cal yr BP to as late as 11,700 cal yr BP, the paleontological record of Homestead Cave indicates a rebound in nearby fish populations (Oviatt, 2014; Broughton and Smith, 2016), signaling a rise in water level in the Great Salt Lake basin as well as a probable return of standing water on the floor of the western Bonneville basin, to a maximum elevation of 1295–1297 m asl (Oviatt et al., 2003, 2005; Oviatt, 2014, 2015; Madsen et al., 2015). This shallow 'Gilbert-episode' lake transgressed at the very end of the Younger Dryas interval (around 11,700 cal yr BP) and regressed to about the level of Great Salt Lake a short time later, perhaps a few decades to a century at most (e.g., Oviatt, 2014; Oviatt, 2015; Oviatt et al., 2015). Water overflowing from Lake Gunnison in the Sevier basin northward into the western Bonneville basin fed a large wetland system in the Old River Bed delta (Oviatt et al., 2003; Madsen et al., 2015; Spencer et al., 2015). Inside Bonneville Estates itself, cool-adapted small mammals such as yellow-bellied marmot (*Marmota flaviventris*), bushy-tailed woodrat (*Neotoma cinerea*), and northern pocket gopher (*Thomomys talpoides*) were recovered (Schmitt and Lupo, 2012). Vegetationally, a continued predominance of pine pollen in sediment cores of the Bonneville basin implies that relatively cool late Pleistocene conditions persisted through the Younger Dryas, but a declining ratio of pine-to-sagebrush pollen suggests gradual aridization (Louderback and Rhode, 2009; Thompson et al., 2016). Woodrat middens dating from the Younger Dryas interval are scarce in the area, but the few records available notably contain shadscale (*Atriplex confertifolia*) in addition to the dominant sagebrush with only trace amounts of limber pine; thus, by this time subalpine conifers had largely retreated to montane uplands (Rhode, 2000, 2016). This period of cool, dry climate is synchronous with the initial pulse of human occupation of the rockshelter after 12,950 cal yr BP as well as subsequent Paleoindian visits through the time of Stratum 18, leading up to the end of the Younger Dryas, 11,700 cal yr BP. Animal remains (especially sage-grouse, pygmy rabbit [*Brachylagus idahoensis*], western longwinged katydid [*Capnobotes occidentalis*], black bear [*Ursus americanus*], and artiodactyls like mountain sheep, deer, and pronghorn) suggest a sagebrush-shadscale steppe environment with isolated conifers (Rhode, 2000a, 2000b) surrounding the shelter, repeatedly attracting humans to Bonneville Estates during this time (Hockett, 2015).

4.2.2. Earliest Holocene (~11,700–10,500 cal yr BP)

Worldwide climate warmed significantly with the close of the Younger Dryas and onset of the Holocene, and the Bonneville basin warmed significantly as well. Whether earliest Holocene climate remained cooler than modern conditions, at least until about 10,000 cal yr BP, is a subject of current debate (Madsen et al. 2001, 2015; Rhode and Louderback, 2015; Steponaitis et al., 2015; Rhode, 2016; Schmitt and Lupo, 2016; Thompson et al., 2016). At least some of the evidence suggesting relatively cool, mesic conditions may actually relate to the persistence of vadose groundwater, seepage which continued to enrich lowland biotic communities in an otherwise increasingly arid environment (Rhode, 2000a, 2016; Oviatt et al., 2015; Rhode and Louderback, 2015; Schmitt and Lupo, 2016; Bradbury et al., 2021). Great Salt Lake regressed from its Gilbert-episode highs immediately after the end of the Younger Dryas, reaching modern Great Salt Lake altitudes and hypersaline conditions shortly after 11,700 cal yr BP and certainly by around 11,500 cal yr BP (Oviatt, 2015; Oviatt et al., 2015; Broughton and Smith, 2016). Despite the disappearance of the shallow Gilbert-episode lake covering the western Bonneville basin floor, substantial wetlands persisted, including in the Old River Bed delta (Madsen et al., 2015), a wetland system supported by overflow from Lake Gunnison until around 11,300 cal yr BP at the latest, and by local groundwater flow after that time. Smaller but still extensive marshes at Fish Springs, Blue Lake, and other localities were likewise fed by a combination of shallow local groundwater and deeper montane-sourced groundwater (Oviatt et al., 2003, 2005, 2015; Reheis et al., 2014; Rhode, 2016; Thompson et al., 2016; Bradbury et al., 2021). Near Homestead Cave, saline-tolerant fish including Utah chub (*Gila atraria*) and mesic-adapted small mammals persisted, again suggesting groundwater-sourced lowland moisture (Grayson, 2000; Broughton and Smith, 2016; Schmitt and Lupo, 2016). Significantly, the Paleoindian (Dry Gulch Phase) occupation of Bonneville Estates continued, albeit with a brief decline ~11,500–11,200 cal yr BP, during this initial episode of early Holocene aridification.

Vegetation in the western Bonneville basin during the earliest Holocene, shown in both local woodrat midden records and regional pollen records, gradually shifted from being sagebrush-dominated to shadscale-dominated shrublands (Rhode, 2000a, 2016; Thompson et al., 2016). The Blue Lake pollen record local to

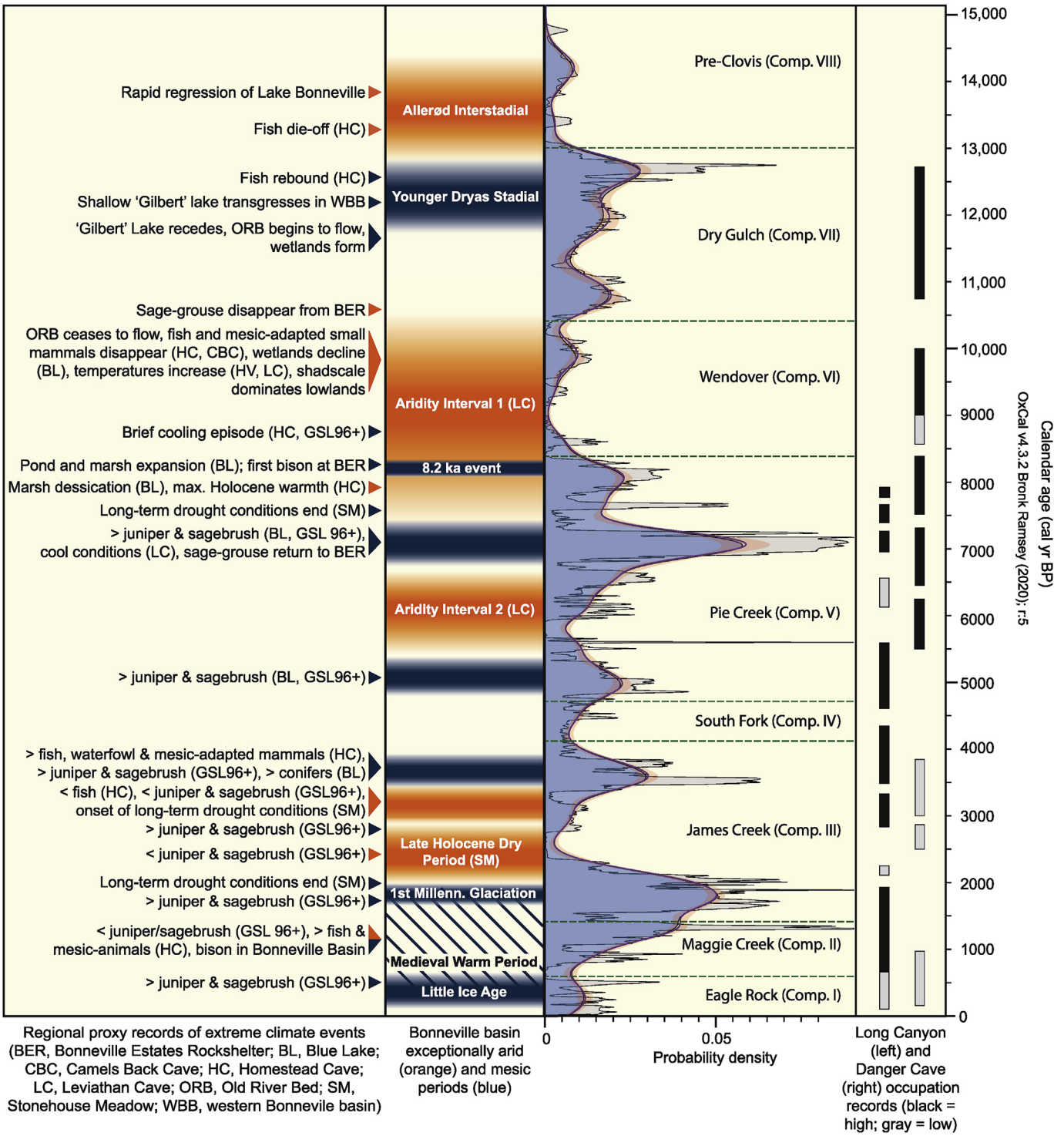

Fig. 8. Comparison of Bonneville Estates Rockshelter's radiocarbon chronology (i.e., summed-probability/kernel-density distribution from Fig. 7) to regional paleoenvironmental proxy records and global climatic events (with blue representing mesic periods, orange representing arid periods, and blue diagonal lines representing a period of strong summer precipitation during otherwise arid times). At far right are comparative archaeological records from Long Canyon (Nevada) and Danger Cave (Utah), showing periods with high (black) and low (gray) occupation rates; periods with no radiocarbon-dated occupations are blank. (For interpretation of the references to colour in this figure legend, the reader is referred to the Web version of this article.)

Bonneville Estates highlights this shift ~11,500 to 10,300 cal yr BP (Louderback and Rhode, 2009), during which Paleoindians continued to regularly visit the rockshelter, partaking in the same subsistence activities as during the latest Pleistocene, centered around fauna of the sagebrush-shrub community (Hockett, 2015). This activity ceased ~10,500 cal yr BP, the time that we interpret represents the local shift to shadscale-dominated shrubland.

4.2.3. Early-mid Holocene (~10,500–8000 cal yr BP)

Environmental conditions outside and inside the rockshelter

changed dramatically in the centuries following 10,000 cal yr BP, as "rapid and severe desertification" (Schmitt and Lupo, 2016) occurred across the Bonneville basin. Water ceased flowing along the Old River Bed 9700 cal yr BP (Oviatt et al., 2003); Great Salt Lake, Blue Lake, and other wetlands declined and in some cases dried completely (Louderback and Rhode, 2009; Thompson et al., 2016); xerophytic shrubs like shadscale dominated low- and middle-elevation slopes at the expense of juniper and even sagebrush, which retreated to higher elevations, between 9500 and 8300 cal yr BP (Louderback and Rhode, 2009; Rhode, 2016; Thompson et al., 2016); and mesic-adapted small mammals disappeared from Homestead Cave and Camels Back Cave by 9300 cal yr BP (Grayson, 2000; Schmitt and Lupo, 2016). In some settings below the level of the Lake Bonneville highstand, however, lake waters trapped in shallow aquifers continued to support mesophilic vegetation such as hackberry (*Celtis reticulata*) and snowberry (*Symphoricarpos longiflorus*) well into the early Holocene (Rhode and Louderback, 2015), but these local conditions were rapidly diminishing as the warming and drying continued. Indeed, a temperature proxy record obtained from oxygen isotopes in hackberry pericarps from Homestead Cave (Rhode and Louderback, 2015; see also Broughton and Smith, 2016) shows elevated temperature at ~9900 cal yr BP. Similarly, stable-isotope ($\delta^{18}O$ and $\delta^{13}C$) values from Leviathan Cave in central Nevada indicate hottest, driest conditions of the Holocene ~9850-7670 cal yr BP, which Lachniet et al. (2020) refer to as 'Aridity Interval 1'.

At Bonneville Estates, after cessation of the Paleoindian occupation ~10,500 cal yr BP, there is very little evidence of human use of the rockshelter, except for a few moments ~10,200–9700 cal yr BP and again briefly 9300 and 8700 cal yr BP when singular hearths and meager archaeological assemblages were deposited. Geologically, the rockshelter's sediments for this period (strata 17b and 17a) are poor in organics and instead characterized by wind-blown silt and sand with rubble from frequent ceiling collapse. The significant aridity, retreat of sagebrush communities to elevations much higher than the rockshelter, and lack of nearby fresh water triggered humans to largely ignore Bonneville Estates for 2200 years, from ~10,500–8300 cal yr BP, especially ~9600-8600 cal yr BP.

The early-mid Holocene in the Bonneville basin, however, does not appear to have been monolithically hot and dry. The isotopic record of temperature from hackberry pericarps at Homestead Cave shows significant variation through the period: cool ~9500 cal yr BP, hot ~9200 cal yr BP, and hotter still ~8000 cal yr BP (Rhode and Louderback, 2015; see also Broughton and Smith, 2016). Pollen spectra from both the Blue Lake and Great Salt Lake (GSL) 96+ cores register similar variation, for example two brief rebounds in sagebrush ~10,000 and again ~8700 cal yr BP (Louderback and Rhode, 2009; Thompson et al., 2016), suggesting cooler conditions briefly. In the GSL 96+ core these are coincident with noticeable increases in juniper, further suggesting more moisture at these times. These apparent cold snaps are synchronous with some of the short-term, ephemeral occupations of the Wendover Phase at Bonneville Estates, ~10,000 and ~8700 cal yr BP.

Global climate records suggest a significant cold snap across the northern hemisphere 8200 cal yr BP (the so-called '8.2 ka event'; Alley et al., 1997); however, Bonneville basin climate proxy records allude to persistent warm, dry conditions at this time. For example, isotopic analyses of speleothems from Lehman Caves, east-central Nevada, signal persistent drought conditions during the 8.2 ka event (Steponaitis et al., 2015), a signal made even more significant given a coeval spike in moisture registered in speleothems in coastal California (Oster et al., 2017). Moreover, the GSL 96+ core (Thompson et al., 2016) shows decreasing juniper and sagebrush and increasing xeric-adapted saltbushes (Amaranthaceae) at this time. The Blue Lake pollen record similarly indicates high relative values of saltbushes, but also high values of grasses, a brief increase in juniper, and signs of a more productive pond/marsh (Louderback and Rhode, 2009). In central Nevada, the Gund Ranch pollen record shows renewed wetlands and increased pine values after ~8500 cal yr BP, following pronounced early Holocene drying, another possible indicator of greater effective moisture during the 8.2 ka event (Brugger and Rhode, 2020). Remarkably, Bonneville Estates' Stratum 16, an organic-rich deposit which signals the onset of a 3500-year-long early Archaic record (Component 5; Pie Creek Phase), has a modeled beginning time of 8299 ± 59 cal yr BP, consistent with the expansion of the pond-marsh mosaic at Blue Lake and statistically coinciding with the global 8.2 ka event. Stratum 16 also yielded the earliest record of Holocene bison (*Bison bison*) in the rockshelter. This could signal that, locally, the 8.2 ka event actually manifested itself in warm and wet, rather than cool and wet, conditions near the shelter if both grasses and bison expanded their ranges or densities at this time (Hockett, 2007). Stratum 16 is also separated stratigraphically from the remainder of Component 5 by a thin layer of silt, sand, and rubble (Stratum 15), suggesting if Stratum 16 represents an episode of ameliorated climate, like the evidence from nearby Blue Lake, it was short-lived and followed by a return to hot, dry conditions. Thus, although the global effects of the brief 8200-cal-yr-BP cold snap appear to have been muted over the Bonneville basin, this pattern may be more apparent than real, given the record developing from Bonneville Estates Rockshelter, nearby Blue Lake, and Gund Ranch in central Nevada.

4.2.4. Middle Holocene (~8000-4000 cal yr BP)

As the middle Holocene dragged on, Bonneville basin climate continued to be relatively hot and dry, but not so hot and dry as during the preceding early-mid Holocene. The Homestead Cave isotopic proxy record for temperature shows maximum warmth at ~8000 cal yr BP, and declining temperature after that (Rhode and Louderback, 2015). Local to Bonneville Estates, the Blue Lake core shows elevated juniper-to-sagebrush + Amaranthaceae ratios compared to before, with higher-than-average spikes (in favor of juniper) specifically at ~7500, 6700, and 5900 cal yr BP (Louderback and Rhode, 2009). The GSL 96+ core registers the same trend, but with elevated spikes (favoring juniper) at 7300, 5900, and 5000 cal yr BP (Thompson et al., 2016). Temporal differences between the two cores' records could be due to regional variation, or the product of differential sampling or chronological modeling (cf. Zimmermann and Wahl, 2020). Suffice it to say, however, in general these records suggest millennial-scale oscillations alternating from relatively cool, moist conditions to hot, dry (i.e., drought) conditions. Farther afield, evidence of cooler, moister climate interdigitated with recurrent drought can be found in the records of Pyramid Lake in western Nevada (Benson et al., 2002; Mensing et al., 2004) as well as Tahoe and Mono lakes in the eastern Sierra (Lindström, 1990; Davis, 1999). Similarly, Leviathan Cave's $\delta^{18}O$ and $\delta^{13}C$ records indicate a 'Cool Oscillation' 7670-6770 cal yr BP followed by a return to significantly dry conditions 6770-5310 cal yr BP ('Aridity Interval 2') (Lachniet et al., 2020).

Bonneville Estates Rockshelter's modeled radiocarbon chronology matches this regional climate record for the middle Holocene rather well. On the one hand, in general the tempo of human occupation 8000-4000 cal yr BP was significantly more rapid than during the preceding early-mid Holocene. On the other hand, this record, which includes components V and IV, is not uniform and instead characterized by a series of peaks and intervening dips in frequency of site occupation. The earliest episode of cool, mesic conditions registered in the pollen records (i.e., 7500/7300 cal yr

BP) is manifested in the Bonneville Estates radiocarbon chronology as the highest, largest peak in the entire record, at ~7300-6800 cal yr BP (early Stratum 14). Leviathan Cave's 'Cool Oscillation' 7670-6770 cal yr BP (Lachniet et al., 2020) overlaps with this strongest pulse in the rockshelter's record as well. Thus, we infer that conditions at the rockshelter were relatively cool and moist at this time (at least relative to earlier Component VI). Not surprisingly, early Stratum 14 chronicles the return of sagebrush-obligate sage-grouse, ending a 3500-year hiatus of this species in the rockshelter (Hockett, 2007, 2015). After this, however, the rate of human occupation dropped considerably and there are signs that the rockshelter may have been abandoned for several centuries, ~5900-5650 cal yr BP. Generally, this period correlates well to Leviathan Cave's 'Aridity Interval 2', 6770-5310 cal yr BP (Lachniet et al., 2020). We hesitate to precisely 'wiggle-match' the records (because of the comparatively coarse-grained chronology of the pollen cores), but point out that minor peaks in the summed-probability/kernel-density distribution generally fall in line with the inferred cool, moist episodes registered in the Blue Lake or GSL 96+ cores. Put simply, following ~7500 cal yr BP, we hypothesize that during the middle Holocene, when upland juniper and sagebrush communities periodically expanded downslope to lower elevations, locally chronicling millennial-scale climate oscillations from hot, dry conditions to cool, moist conditions, the rockshelter became an attractive subsistence base to humans. Conversely, during intervening periods of prolonged drought and the retreat of these upland communities, the rockshelter witnessed significantly fewer visits. Eventually, with improved chronological control over the eastern Great Basin's pollen records and completion of analyses of the rockshelter's paleoecological and archaeological assemblages, we expect to be able to better test this relationship.

4.2.5. Early-late Holocene (~4000-1500 cal yr BP)

Traditionally the late Holocene in the eastern Great Basin is considered to have started ~4500-4000 cal yr BP, with the onset of cooler, wetter 'neo-pluvial' or 'neo-glacial' conditions (e.g., Grayson, 2011; Hockett, 2015; Schmitt and Lupo, 2016). The region's paleoenvironmental records, however, indicate that during this time climate continued to swing between marked pluvial events with relatively high lake levels and major droughts when moisture became scarce. Mehringer (1977; 1985), following Antevs (1948; 1955) and Morrison (1965), relying on stratigraphic and microfossil evidence associated with a small set of bulk-sediment radiocarbon dates, hypothesized that starting about 3800 cal yr BP Great Salt Lake expanded to an elevation sufficiently high (~1287 m or even higher) to cause flooding into the western Bonneville basin (Grayson, 2011). The Homestead Cave paleontological record of fish and small mammals from Stratum XII supports such a late Holocene 'neopluvial' episode: Utah chub reappears in the record in a deposit dated to 3830-3550 cal yr BP (Broughton and Smith, 2016), while long-tailed pocket mouse (*Chaetodipus formosus*) returns after a 4000-year hiatus and Western harvest mouse (*Reithrodontomys megalotis*), attracted to well-watered habitats, increases in numbers (Grayson, 2000; Schmitt and Lupo, 2016). The GSL 96+ pollen core similarly records a synchronous (3800-cal-yr-BP) spike in juniper and sagebrush indicating wetter and cooler conditions than during the middle Holocene (Thompson et al., 2016).

Both the duration and magnitude of this pluvial event, however, have been debated. Oviatt et al. (2021, in press) caution that such a neopluvial expansion of Great Salt Lake remains poorly constrained chronologically and the lake would likely have been subject to rapid fluctuations in level, similar to its historic hydrograph. Mehringer (1977) originally interpreted a high lake span of 3800–2200 cal yr BP, Madsen et al. (2001) suggested a shorter span of 3100–2450 cal yr BP, and Grayson (2011) a span of 3600–2000 cal yr BP. Madsen et al. (2001) further suggested a maximum lake level of ~2184 m (consistent with brief historic highs), which likely would not have reached the Great Salt Lake Desert. Mensing et al. (2013) have recently argued that the episode was much more short-lived, regarding Mehringer's original bulk-sediment dates as unreliable. The GSL 96+ pollen record confirms this, indicating a sharp decline in juniper and sagebrush ~3400-3200 cal yr BP, a response to significantly hotter, dryer conditions (Thompson et al., 2016). Moreover, at Homestead Cave the accumulation of fish remains ceased before the deposition of Stratum XV (Broughton and Smith, 2016), which we interpret to have begun by 3000 cal yr BP. Thus, based on these proxy records, the first pluvial event of the late Holocene in the Bonneville basin spanned from only 3900 to ~3400 cal yr BP. Coincident with this first pluvial event of the late Holocene at Bonneville Estates is one of the highest peaks in its radiocarbon probability density, lower Component 3 of the early James Creek Phase, ~4000-3400 cal yr BP.

Following this first major pluvial event of the late Holocene, regional climate swung between relatively hot, dry and cool, wet conditions. This is evident in the GSL 96+ record: warm, dry conditions 3400-3000 cal yr BP, strong pluvial conditions 3000-2600 cal yr BP, drought 2700-2000 cal yr BP, and moderate pluvial conditions 2000-1700 cal yr BP (Thompson et al., 2016). Thompson et al. (2016:280) tentatively correlated the 2000-1700 cal-yr-BP pluvial episode to the globally-recognized 'First Millennium Glaciation'. Homestead Cave's paleontological record for this time is more muted, with Stratum XV reflecting generally arid conditions 3000 to ~1600 cal yr BP (Grayson 2000; Broughton and Smith, 2016). Farther west in central Nevada, pollen records from Stonehouse Meadow, Mission Cross Bog, Kingston Meadow, and Newark Valley provide a repeated pattern for a series of droughts similar to the GSL 96+ core (Mensing et al. 2008, 2013), and they are evident in tree-ring data from western Nevada, too (Millar et al., 2018). In particular, Stonehouse Meadow demonstrates a major episode of persistent, long-term drought ~2800-1850 cal yr BP, the 'Late Holocene Dry Period' (Mensing et al. 2008, 2013), roughly coeval with the second late Holocene GSL 96+ drought. Bonneville Estate's radiocarbon record for the middle and late James Creek Phase (Component 3) closely follows these trends, with a major decline in human occupation ~3400-3200 cal yr BP, a minor occupation peak ~3200-2700 cal yr BP, a significant lack of occupation 2700-2300 cal yr BP, and a major pulse of occupation from ~2300 to 1550 cal yr BP, near the end of the James Creek Phase. Without question, there is strong agreement between regional climate oscillations and the rockshelter's occupation record during the James Creek Phase.

4.2.6. Late-late Holocene (~1500-150 cal yr BP)

Proxy environmental records for the final 1500 years of prehistory indicate continued climatic oscillations between hot, dry and cool, wet conditions. The GSL 96+ record suggests a period of long-term drought ~1700-600 cal yr BP (Thompson et al., 2016), and this is corroborated by synchronous drought conditions inferred at Stonehouse Meadow, ~1300-700 cal yr BP (Mensing et al. 2008, 2013). In the GSL 96+ core this was followed by strong pluvial conditions after 600 cal yr BP, which Thompson et al. (2016:280) attributed to the 'Little Ice Age'. Contrary to this, however, is Homestead Cave's paleontological record for the period of ~1250-800 cal yr BP, preserved in strata XVI and XVII, which registers the reappearance of Utah chub and little pocket mouse (*Perognathus parvas*) (Grayson 2000; Broughton and Smith, 2016), both indicators of pluvial conditions at a time when the GSL 96+ and Stonehouse Meadow cores suggest prolonged drought. Dating of the Homestead Cave deposits, however, is based on just two

radiocarbon ages, both of them older than the youngest acceptable ages for underlying Stratum XV. This stratigraphic reversal in chronology weakens the Homestead Cave record for this period, but other regional proxy records suggest that this was a period of increased *summer* rainfall, episodically promoting the growth of grasses and expansion of bison populations in the eastern Great Basin (Lupo and Schmitt, 1997; Grayson, 2006). Within the western Bonneville basin specifically, nearly all dated bison remains fall within this period (Hockett and Morgenstein, 2003), making the inferred summer precipitation pattern especially evident.

Significantly, the Component 2 occupation assigned to the Maggie Creek Phase, ~1400-850 cal yr BP, falls squarely within this period of increased summer rainfall. Culturally, this coincides with the regional advent of bow-and-arrow technology, and in the Goshute-Deep Creek area nearby Bonneville Estates Rockshelter, multiple archaeological occupations suggest a local resident population, with some material-culture remains even suggesting the nearby presence of part-time maize horticulturalists (i.e., the Fremont culture) (Buck et al., 2002; Janetski, 2004; Madsen and Schmitt, 2005). Within Bonneville Estates, Component 2 deposits have yielded remains of bison as well as a few kernels of maize, corroborating the interpretation of an expansion of bison (and human horticulturalists) 1400-850 cal yr BP, during a summer-wet interval, not a drought.

The final climatic phase of the late Holocene, the Little Ice Age, is evident in the GSL 96+ core as a period of cool, mesic conditions after 600 cal yr BP (Thompson et al., 2016). At Bonneville Estates, this is coeval with the minor peak in radiocarbon probability density associated with Component 1, the rockshelter's Eagle Rock Phase occupation starting ~530 cal yr BP.

4.3. Comparison with nearby Bonneville basin archaeological records

Mobile hunter-gatherers operated on a larger scale than a single site like Bonneville Estates Rockshelter affords, so full understanding of the process of cultural evolution in arid contexts like the western Bonneville basin can only be achieved regionally. Most notably, spring-based or marsh-based residential locations, even in low-elevation settings, will likely yield different histories relative to long-term regional environmental fluctuations than mid-elevation camps away from springs (e.g., Thomas, 2020). Similarly, high-elevation sites in cooler, more mesic settings will provide different histories of logistical foraging than sites like Bonneville Estates. During xeric episodes, base camps would have become established close to springs and creeks, while during more mesic episodes, humans were potentially free to establish camps farther from such reliable water sources, at places like Bonneville Estates. Therefore, we call attention to two important archaeological sites (or site clusters) nearby Bonneville Estates Rockshelter — Danger Cave (Utah) and Long Canyon (Nevada) — both located adjacent to perennial springs and both yielding relatively large radiocarbon datasets (Fig. 8).

Danger Cave is situated adjacent to a spring-fed playa-margin marsh on the floor of the western Bonneville basin, 30 km north of Bonneville Estates (Jennings, 1957; Oviatt et al., 2018; Rhode and Madsen, 1998; Rhode et al., 2005, 2006). Its chronology (based on a sample of 57 radiocarbon ages) proceeds similarly to Bonneville Estates, but with two obvious and major differences. First and foremost, the Wendover Phase is well-represented with multiple occupation events evident 10,000–8600 cal yr BP, indicating that even though humans rarely visited Bonneville Estates during this time, they frequently occupied Danger Cave, likely employing it as a base camp throughout the early-mid Holocene (Rhode et al., 2006). Second, after 5500 cal yr BP, there is little evidence of human occupation of Danger Cave in the radiocarbon record, but this is likely because the cave's opening had become quite small by that time so that it lost much of its attractiveness to humans (Madsen, 2014). Other nearby cave sites (e.g., Juke Box Cave; Jennings 1957) likely contain records of later occupations.

At Long Canyon, located near extensive Big Springs in the higher-elevation sagebrush-shrubland and juniper-woodland setting of neighboring Goshute Valley, 60 km northwest of Bonneville Estates (Cunnar et al., 2019), dozens of archaeological sites have yielded a chronology of human occupation based on more than 244 radiocarbon ages. Much of Long Canyon's radiocarbon distribution matches Bonneville Estates', except that Dry Gulch and Wendover occupations predating 8400 cal yr BP are completely lacking from the Long Canyon radiocarbon record. Possibly this absence is because early archaeological contexts around the springs were more deeply buried than rescue excavations permitted, but in our own surveys elsewhere in the Goshute Valley, Paleoindian projectile points including Western Stemmed varieties occur only rarely in undated surface contexts, typically as isolated finds. After 8400 cal yr BP, the Long Canyon record shows similar trends as Bonneville Estates, especially regarding low occupation rates and even occupation breaks during more warm, arid times, albeit these appear to have been briefer at Long Canyon than at the rockshelter.

These variable records for Bonneville Estates, Danger Cave, and Long Canyon reflect changes in residential options as humans adapted to environmental changes playing out at a regional scale. They demonstrate the need for the development of a detailed, comprehensive regional chronology of human occupation for the western Bonneville basin and neighboring smaller, higher-elevation valleys to the west, a database of radiocarbon-dated events reflecting all of the subsistence-settlement choices available to humans in the region since 13,000 cal yr BP. This will take a concerted effort that includes re-analysis of previously excavated sites as well as excavations at newly discovered or understudied locations.

5. Summary and conclusions

Throughout the Holocene, oscillating climatic intervals in the western Bonneville basin of western North America challenged human settlement, even among the traditional hunter-gatherers who long occupied it (Steward, 1938). As such, the region's paleoecological and archaeological records can serve as an important case study of how humans successfully adjust to severe climate and environmental change, in this case repeated oscillations between prolonged warm 'drought' conditions and cool 'pluvial' conditions. Perched on the high shoreline of Pleistocene Lake Bonneville, at 1582 m above sea level, Bonneville Estates Rockshelter has long straddled an important vegetation ecotone in this desert setting — the transition from upland-sagebrush to lowland-shadscale desert-shrub communities. In this position, 8 km from the nearest sources of fresh water, we have established a 13,000-year-long record of human occupation that strongly correlates to local environmental change, brought on by larger-scale regional climate change (Fig. 8).

At the start of the record, the rockshelter's rich Paleoindian component ~12,950–10,500 cal yr BP reveals repeated human occupations during the stadial conditions of the Younger Dryas as well as continued cool, arid conditions in the earliest Holocene, until the region's playas and marshes became perennially dry and plant and animal resources became locally scarce. From ~10,500 to ~8400 cal yr BP, humans rarely visited Bonneville Estates as the region witnessed nearly 2000 years of drought — the Aridity Interval 1 of the Leviathan Cave isotope record — and extirpations of mesic-adapted animals in low-elevation settings. Coincident with the '8.2 ka' cold snap, the rockshelter witnessed its first major pulse

of early Archaic human occupation, and occupation intensity fluctuated thereafter through the middle Holocene, ~8000 to ~4000 cal yr BP. These millennial-scale fluctuations correlate to a series of climatic oscillations between cool, mesic conditions and warm, arid conditions, which led to the elevational expansions and contractions of upland sagebrush-shrub and juniper-woodland communities in mid-elevation settings like Bonneville Estates. During cool, mesic times local foragers made the rockshelter a regular base from which they could carry out subsistence activities, while during warm, arid times, their visits became rarer and briefer, and at times even ceased for centuries. Especially noteworthy was a prolonged period of drought — Aridity Interval 2 in the Leviathan Cave record — when from ~5900 to 5700 cal yr BP, human occupation of the rockshelter all but ceased. These oscillations continued into the early part of the late Holocene (~4000-1500 cal yr BP), when transpired some of the most dramatic swings in regional climate and environment as well as human occupation of Bonneville Estates. One of these was a period of prolonged drought (the Late Holocene Dry Period, ~2800-1900 cal yr BP) that saw possible abandonment of the rockshelter ~2800-2400 cal yr BP. Another is the subsequent pluvial episode referred to globally as the First Millennium Glaciation, which registered one of the most intense periods of human occupation of the rockshelter, ~2000-1500 cal yr BP. Following this occupation peak human groups continued their frequent and repeated visits to Bonneville Estates during a relatively warm period ~1400-850 cal yr BP that featured increased summer precipitation and greater abundance of grasses and bison in the Bonneville basin. The sequence ends, finally, with regionally cool, mesic climate during the Little Ice Age and moderate occupation intensity of the rockshelter, after 530 cal yr BP.

Despite the large excavation and comprehensive suite of radiocarbon ages for Bonneville Estates Rockshelter, we recognize that there may be other explanations for the resulting radiocarbon distribution. Sampling could still be an issue. If excavations and dating continued, we could potentially close some of the gaps and raise some of the valleys in the distribution; however, continued dating of the already excavated materials will not significantly change the distribution. Similarly, some may take exception to our interpretation that peaks and valleys in the probability density represent variable occupation intensity (i.e., change in the frequency of visits to the rockshelter per unit time). Peaks in the record alternatively could represent more intensive activity being carried out during the same number of occupations, creating more opportunities for us to date individual occupation episodes and artificially creating the peaks. This is why we focused on the dating of fire hearths, the materials we considered to be the best proxy for quantifying the number of human visits, or overnight stays, at the rockshelter. Even if the peak distributions of radiocarbon ages based on number of hearths do not correlate precisely with increased number of visits, this proxy measure still indicates more people occupying the shelter per visit during these peak times, another indication of more intense use of the nearby landscape by humans during these mesic climatic episodes. If radiocarbon ages obtained from other cultural debris (e.g., coprolites, point binding, baskets, and cordage) are removed from the analysis, the overall distribution would not change significantly, with the highest peaks becoming slightly diminished and the gaps only widening, if they change at all.

Thus, the adaptive flexibility evident in the human record of occupation at Bonneville Estates Rockshelter demonstrates the ability of Great Basin foragers to make the necessary changes to respond to multiple episodes of short-term and long-term climatic changes, some of them extreme, attesting to an intimate knowledge of their natural and cultural circumstances for survival. The highly correlative record of archaeology and climate presented here cannot be dismissed as coincidental. Further chronicling and explaining this symbiotic relationship will continue to be a major line of scientific inquiry at Bonneville Estates Rockshelter and across the western Bonneville basin for years to come.

Author statement

Goebel directed the Bonneville Estates Rockshelter excavation in 2000–2009, and he has continued to serve as the research team's coordinator since then. He developed the concept for this paper, conducted the chronological analyses presented, and prepared the original draft and figures. Bryan Hockett, David Rhode, and Kelly Graf co-directed the field project and respectively have managed zooarchaeological, archaeobotanical, and stratigraphic/sedimentological analyses. Hockett and Goebel analyzed the bifacial-point assemblage presented. During the past 20 years, all four authors contributed to the creation of the radiocarbon database presented, selecting and preparing samples, and compiling and interpreting results; however, Rhode taxonomically identified nearly all of the dated plant macrofossils while Hockett identified the dated bones. During 2020–2021, Hockett, Rhode, and Graf contributed significantly to the editing and revising of the manuscript, which Goebel managed. The project truly has been a team effort since day one.

Declaration of competing interest

The authors declare the following financial interests/personal relationships which may be considered as potential competing interests: Ted Goebel and Kelly Graf are a married couple. Both are tenured members of the faculty of Texas A&M University (Goebel, professor; Graf, associate professor). They have worked together with Hockett and Rhode on this project since its inception in 1999.

Acknowledgements

Cassandra Albush and Marion Coe assembled and prepared coprolite and textile samples for dating, respectively. Geoffrey Smith provided funding for dating the two samples of bifacial-point binding. Brendan Culleton, David Carlson, and Tom Higham offered invaluable guidance using OxCal early on in this project. Stephen Kuehn provided the geochemical analysis of the Mazama tephra reported in Table S3. Special thanks to C.G. (Jack) Oviatt and another anonymous reviewer for their helpful, positive comments on an earlier version of the paper. The large series of radiocarbon dates was paid for through support from the U.S. National Science Foundation, U.S.D.I. Bureau of Land Management, Sundance Archaeological Research Fund at the University of Nevada Reno, and Endowed Professorship for First American Studies at Texas A&M University.

Appendix A. Supplementary data

Supplementary data to this article can be found online at https://doi.org/10.1016/j.quascirev.2021.106930.

References

Albush, C.J., 2010. Prehistoric Diet at Bonneville Estates Rockshelter, Nevada. M.A. thesis, University of Nevada, Reno.
Alley, R.B., Mayewski, P.A., Sowers, T., Stuiver, M., Taylor, K.C., Clark, P.U., 1997. Holocene climatic instability: a prominent, widespread event 8200 yr ago. Geology 25, 483–486.
Antevs, E., 1948. Climatic Changes and Pre-white Man, vol. 38. University of Utah Bulletin, pp. 167–191.
Antevs, E., 1955. Geologic-climatic dating in the west. Am. Antiq. 20, 317–335.
Bamforth, D.B., Grund, B., 2012. Radiocarbon calibration curves, summed probability distributions and early Paleoindian population trends in North America.

J. Archaeol. Sci. 39, 1768–1774.
Benson, L., Burdett, J., Lund, S., Kashgarian, M., Mensing, S., 1997. Nearly synchronous climate change in the northern hemisphere during the last glacial termination. Nature 388, 263–265.
Benson, L., Kashgarian, M., Rye, R., Lund, S., Paillet, F., Smooth, J., Kester, C., Mensing, S., Meko, D., Lindström, S., 2002. Holocene multidecadel and multicentennial droughts affecting northern California and Nevada. Quat. Sci. Rev. 21, 659–682.
Benson, L.V., Currey, D.R., Dorn, R.I., Lajoie, K.R., Oviatt, C.G., Robinson, S.W., Smith, G.I., Stine, S., 1990. Chronology and expansion of Four Great Basin lake systems during the past 35,000 years. Palaeogeography, Paleoclimatology, Palaeoecology 78, 241–286.
Benson, L., Burdett, J., Lund, S., Kashgarian, M., Mensing, S., 2007. Nearly synchronous climate change in the northern hemisphere during the last glacial termination. Nature 388, 263–265.
Benson, L.W., Pauketat, T.R., Cook, E.R., 2009. Cahokia's boom and bust in the context of climate change. Am. Antiq. 74, 467–483.
Bradbury, C.D., Jewell, P.W., Fernandez, D.P., Lerback, J.C., DeGraffenried, J.V., Peterson, E.U., 2021. Water provenance at the Old River Bed inland delta and ground water flow from the Sevier basin of central Utah during the Pleistocene-Holocene transition. Quat. Res. 99, 114–127.
Bronk Ramsey, C., 2009. Bayesian analysis of radiocarbon dates. Radiocarbon 5, 337–360.
Bronk Ramsey, C., 2017. Methods for summarizing radiocarbon datasets. Radiocarbon 59, 1809–1833.
Broughton, J.M., Smith, G.R., 2016. The fishes of Lake Bonneville: implications for drainage history, biogeography, and lake levels. In: Oviatt, C.G., Shroder, J.F. (Eds.), Lake Bonneville: A Scientific Update. Developments in Earth Surface Processes, vol. 20. Elsevier, pp. 292–351.
Brugger, S.O., Rhode, D., 2020. Impact of Pleistocene-Holocene climate shifts on vegetation and fire dynamics and its implications for Prearchaic humans in the central Great Basin, USA. J. Quat. Sci. https://doi.org/10.1002/jqs.3248.
Buck, P., Hockett, B., Graf, K., Goebel, T., Griego, G., Perry, L., Dillingham, E., 2002. Oranjeboom Cave: a single-component Eastgate site in northeast Nevada. Utah Archaeology 15, 99–112.
Burley, D.V., Edinborough, K., 2014. Discontinuity in the Fijian archaeological record supported by a Bayesian radiocarbon model. Radiocarbon 56, 295–303.
Chamberlin, R.V., 1911. Part 5. The Ethno-Botany of the Gosiute Indians of Utah. Memoirs of the American Anthropological Association, vol. II. The New Era Printing Company.
Coe, M.M., 2020. Reconstructing Identity in the Bonneville Basin: Holocene-Aged Cordage and Coiled Basketry from the Eastern Great Basin. Ph.D. dissertation, Texas A&M University, College Station, TX.
Contreras, D.A., Meadows, J., 2014. Summed radiocarbon calibrations as a population proxy: a critical evaluation using a realistic simulation approach. J. Archaeol. Sci. 52, 591–608.
Cunnar, G., Stoner, E., Wheeler, C., Brockway, R., 2019. Treatment and Data Recovery of 130 Sites at the Long Canyon Mine, Elko County, Nevada. Report. Bureau of Land Management, Elko, NV, pp. 1–3257.
Currey, D.R., 1990. Quaternary palaeolakes in the evolution of semidesert basins, with special emphasis on Lake Bonneville and the Great Basin, U.S.A. Palaeogeography. Palaeoclimatology, Palaeoecology 76, 189–214.
Davis, O.K., 1999. Pollen analysis of a late-glacial and Holocene sediment core from Mono Lake, Mono County, California. Quat. Res. 52, 243–249.
Egan, J., Staff, R., Blackford, J., 2015. A high-precision age estimate of the Holocene Plinian eruption of Mount Mazama, Oregon, USA. Holocene 25, 1054–1067.
Elston, R.G., Budy, E.E., 1990. The Archaeology of James Creek Shelter. Anthropological Papers No. 115. University of Utah Press, Salt Lake City.
Gilbert, G.K., Lake Bonneville. Monographs of the United States Geological Survey 1. Government Printing Office, Washington.
Goebel, T., 2007. Pre-Archaic and Early Archaic Technological Activities at Bonneville Estates Rockshelter: A First Look at the Lithic Artifact Record. In: Graf, K.E., Schmitt, D.N. (Eds.), Paleoindian or Paleoarchaic? Great Basin Human Ecology at the Pleistocene-Holocene Transition. University of Utah Press, Salt Lake City, pp. 156–184.
Goebel, T., Hockett, B., Adams, K.D., Rhode, D., Graf, K., 2011. Climate, environment, and humans in North America's Great Basin during the Younger Dryas, 12,900-11,600 calendar years ago. Quat. Int. 242, 479–501.
Graf, K.E., 2007. Stratigraphy and chronology of the Pleistocene to Holocene transition at Bonneville Estates Rockshelter, eastern Great Basin. In: Graf, K.E., Schmitt, D.N. (Eds.), Paleoindian or Paleoarchaic: Great Basin Human Ecology at the Pleistocene-Holocene Transition. University of Utah Press, Salt Lake City, pp. 82–104.
Grayson, D.K., 2000. Mammalian responses to middle Holocene climatic change in the Great Basin of the western United States. J. Biogeogr. 27, 181–192.
Grayson, D.K., 2006. Holocene bison in the Great Basin, western USA. Holocene 16, 913–925.
Grayson, D.K., 2011. The Great Basin: A Natural Prehistory. University of California Press, Berkeley.
Higham, T., Jacobi, R., Basell, L., Bronk Ramsey, C., Chiotti, L., Nespoulet, R., 2016. Precision dating of the Palaeolithic: a new radiocarbon chronology for the Abri Pataud (France), a key Aurignacian sequence. J. Hum. Evol. 61, 549–563.
Hildebrandt, W., McGuire, K., King, J., Ruby, A., Young, D.C., 2016. Prehistory of Nevada's Northern Tier: Archaeological Investigations along the Ruby Pipeline. American Museum of Natural History Anthropological Papers, No. 101, New York.
Hockett, B., 2007. Nutritional ecology of late Pleistocene to middle Holocene subsistence in the Great Basin: zooarchaeological evidence from Bonneville Estates Rockshelter. In: Graf, K.E., Schmitt, D.N. (Eds.), Paleoindian or Paleoarchaic: Great Basin Human Ecology at the Pleistocene-Holocene Transition. University of Utah Press, Salt Lake City, pp. 204–230.
Hockett, B., 2015. The zooarchaeology of Bonneville Estates Rockshelter: 13,000 years of Great Basin hunting strategies. J. Archaeol. Sci.: Report 2, 291–301.
Hockett, B., Goebel, T., 2019. The projectile points from Bonneville Estates Rockshelter: description of two new point types and implications for the long and short chronology debate in the Great Basin. Nevada Archaeologist 31, 9–50.
Hockett, B., Morgenstein, M., 2003. Ceramic production, Fremont foragers, and the late Archaic prehistory of the north-central Great Basin. Utah Archaeology 16, 1–36.
Hostetler, S.W., Giorgi, F., Bates, G.T., Bartlein, P.J., 1994. Lake-atmosphere feedbacks associated with paleolakes Bonneville and Lahontan. Science 263, 665–668.
Janetski, J.C., 2004. 2003 Test Excavations at Mosquito Willie (42TO137). Brigham Young University Museum of Peoples and Cultures Technical Series No. 04-12, Provo, UT.
Jennings, J.D., 1957. Danger Cave. University of Utah Anthropological Papers No. 27. University of Utah, Salt Lake City.
Jennings, J.D., 1986. Prehistory: Introduction. In: d'Azevedo, W.L. (Ed.), Great Basin, Vol. 11, Handbook of North American Indians. Smithsonian Institution, Washington, DC, pp. 113–119.
Kelly, R.L., 2001. Prehistory of the Carson Desert and Stillwater Mountains: Environment, Mobility, and Subsistence in a Great Basin Wetland. Anthropological Papers No. 123. University of Utah Press, Salt Lake City.
Kelly, R.L., Surovell, T.A., Shuman, B.N., Smith, G.M., 2013. A continuous climatic impact on Holocene human populations in the Rocky Mountains. Proc. Natl. Acad. Sci. Unit. States Am. 110, 443–447.
Kennett, D.J., Breitenbach, S.F., Aquino, V.V., Asmerom, Y., Awe, J., Baldini, J.U.L., Bartlein, P., Culleton, B.J., Ebert, C., Jazwa, C., Macri, M.J., Marwan, N., Polyak, V., Prufer, K.M., Ridley, H.E., Sodemann, H., Winterhalder, B., Haug, G.H., 2012. Development and disintegration of Maya political systems in response to climate change. Science 338, 788–791.
Lachniet, M.S., Denniston, R.F., Asmerom, Y., Polyak, V.J., 2014. Orbital control of western North America atmospheric circulation and climate over two glacial cycles. Nat. Commun. 5, 3805.
Lachniet, M.S., Asmerom, Y., Polyak, V., Denniston, R., 2020. Great Basin paleoclimate and aridity linked to arctic warming and tropical Pacific sea surface temperatures. Paleooceanography and Paleoclimatology 34, e2019PA003785.
Lindström, S., 1990. Submerged tree stumps as indicators of mid-Holocene aridity in the Lake Tahoe basin. J. Calif. Great Basin Anthropol. 12, 146–157.
Louderback, L.A., Rhode, D.E., 2009. 15,000 years of vegetation change in the Bonneville basin: the Blue Lake pollen record. Quat. Sci. Rev. 28, 308–326.
Louderback, L.A., Grayson, D.K., Llobera, M., 2011. Middle-Holocene climates and human population densities in the Great Basin, western USA. Holocene 21, 366.
Lupo, K.D., Schmitt, D.N., 1997. On late Holocene variability in bison populations in the northeastern Great Basin. J. Calif. Great Basin Anthropol. 19, 50–69.
Lyle, M., Heusser, L., Ravelo, C., Yamamoto, M., Barron, J., Diffenbaugh, N.S., Herbert, T., Andreasen, D., 2012. Out of the tropics: the Pacific, Great Basin lakes, and late Pleistocene water cycle in the western United States. Science 337, 1629–1633.
Madsen, D.B., 2014. Eight decades of easting dust: a short history of archaeological research at Danger Cave. In: Janetski, J., Parezo, N. (Eds.), Archaeology for All Times: Papers in Honor of Don D. Fowler. University of Utah Press, Salt Lake City, pp. 191–201.
Madsen, D.B., Schmitt, D.N., 2005. Buzz-Cut Dune and Fremont Foraging at the Margin of Horticulture. University of Utah Anthropological Papers Number 124. University of Utah Press, Salt Lake City.
Madsen, D.B., Rhode, D., Grayson, D.K., Broughton, J.M., Livingston, S.D., Hunt, J., Quade, J., Schmitt, D.N., Shaver III, M.W., 2001. Late Quaternary environmental change in the Bonneville basin, western USA. Palaeogeogr. Palaeoclimatol. Palaeoecol. 167, 243–271.
Madsen, D.B., Schmitt, D.N., Page, D., 2015. The Paleoarchaic Occupation of the Old River Bed Delta. University of Utah Anthropological Papers No. 128, University of Utah Press, Salt Lake City.
Martindale, A., Morlan, R., Betts, M., Blake, M., Gajewski, K., Gajewski, M., Chaput, M., Mason, A., Vermeersch, P., 2016. Canadian Archaeological Radiocarbon Database (CARD 2.1). https://www.canadianarchaeology.ca.
McGee, D., Moreno-Chamarro, E., Marshall, J., Galbraith, E.D., 2018. Western U.S. lake expansions during Heinrich stadials linked to Pacific Hadley circulation. Science Advances 4, eaav0118.
McGuire, K.R., Delacorte, M.G., Carpenter, K., 2004. Archaeological Excavations at Pie Creek and Tule Valley Shelters, Elko County, Nevada. Anthropological Papers No. 25. Nevada State Museum, Carson City.
Mehringer, P.J., 1977. Great Basin late Quaternary environments and chronology. In: Fowler, D.D. (Ed.), Models of Great Basin Prehistory. Desert Research Institute Publications in Social Science, University of Nevada, Reno, pp. 113–167.
Mehringer, P.J., 1985. Late-Quaternary pollen records from the interior Pacific Northwest and northern Great Basin of the United States. In: Bryant, V.M. (Ed.), Pollen Records of Late-Quaternary North American Sediments. American Association of Stratigraphic Palynologists, Dallas, pp. 167–189.
Mensing, S.A., Benson, L.V., Kashgarian, M., Lund, S., 2004. A Holocene pollen record of persistent droughts from Pyramid Lake, Nevada, USA. Quat. Res. 62, 29–38.

Mensing, S., Smith, J., Norman, K.B., Allan, M., 2008. Extended drought in the Great Basin of western North America in the last two millennia reconstructed from pollen records. Quat. Int. 188, 78–89.
Mensing, S.A., Sharpe, S.E., Tunno, I., Sada, D.W., Thomas, J.M., Starratt, S., Smith, J., 2013. The late Holocene dry period: multiproxy evidence for an extended drought between 2800 and 1850 cal yr BP across the central Great Basin, USA. Quat. Sci. Rev. 78, 266–282.
Millar, C.I., Charlet, D.A., Delany, D.L., King, J.C., Westfall, R.D., 2018. Shifts of demography and growth in limber pine forests of the Great Basin, USA, across 4000 yr of climate variability. Quat. Res. 91, 691–704.
Morrison, R.B., 1965. Lake Bonneville: Quaternary Stratigraphy of Eastern Jordan Valley, South of Salt Lake City, Utah. Geological Survey Professional Paper 477. United States Geological Survey, Government Printing Office, Washington.
Oster, J.L., Sharp, W.D., Covey, A.K., Gibson, J., Rogers, B., Mix, H., 2017. Climate response to the 8.2 ka even in coastal California. Sci. Rep. 7, 3886.
Oviatt, C.G., 1997. Lake Bonneville fluctuations and global climate change. Geology 25, 155–158.
Oviatt, C.G., 2014. The Gilbert Episode in the Great Salt Lake Basin, Utah. Miscellaneous Publication No. 14-3. Utah Geological Survey, Salt Lake City.
Oviatt, C.G., 2015. Chronology of Lake Bonneville, 30,000 to 10,000 yr B.P. Quat. Sci. Rev. 110, 166–171.
Oviatt, C.G., 2020. G.K. Gilbert and the Bonneville shoreline. Geology of the Intermountain West 7, 301–320.
Oviatt, C.G., Jewell, P.W., 2016. The Bonneville Shoreline: reconsidering Gilbert's interpretation. In: Oviatt, C.G., Shroder, J.F. (Eds.), Lake Bonneville: A Scientific Update. Developments in Earth Surface Processes, 20. Elsevier, Amsterdam, pp. 88–104.
Oviatt, C.G., Shroder, J.F. (Eds.), 2016. Lake Bonneville: A Scientific Update. Elsevier, Amsterdam.
Oviatt, C.G., Currey, D.R., Sack, D., 1992. Radiocarbon chronology of Lake Bonneville, eastern Great Basin, USA. Palaeogeogr. Palaeoclimatol. Palaeoecol. 99, 225–241.
Oviatt, C.G., Madsen, D.B., Schmitt, D.N., 2003. Late Pleistocene and early Holocene rivers and wetlands in the Bonneville basin of western North America. Quat. Res. 60, 200–210.
Oviatt, C.G., Miller, D.M., McGeehiin, J.P., Zachary, C., Mahan, S., 2005. The Younger Dryas phase of Great Salt Lake, Utah, USA. Palaeogeogr. Palaeoclimatol. Palaeoecol. 219, 263–284.
Oviatt, C.G., Madsen, D.B., Miller, D.M., Thompson, R.S., McGeehin, J.P., 2015. Early Holocene Great Salt Lake, USA. Quat. Res. 84, 57–68.
Oviatt, C.G., Pigati, J.S., Madsen, D.B., Rhode, D.E., Bright, J., 2018. Juke Box Trench: A Valuable Archive of Late Pleistocene and Holocene Stratigraphy in the Bonneville Basin. Utah. Utah Geological Survey Miscellaneous Publication 18-1, Salt Lake City.
Oviatt, C.G., Atwood, G., Thompson, R.S., 2021. History of Great Salt Lake, Utah, USA, since the termination of Lake Bonneville. In: Rosen, M.R., Park-Bousch, L., Finkelstein, D.B. (Eds.), Limnogeology: Progress, Challenges and Opportunities: A Tribute to Beth Gierlowski-Kordesch. Springer (in press).
Reheis, M.C., Adams, K.D., Oviatt, C.G., Bacon, S.N., 2014. Pluvial lakes in the Great Basin of the western United States—a view from the outcrop. Quat. Sci. Rev. 97, 33–57.
Reimer, P., Austin, W., Bard, E., Bayliss, A., Blackwell, P., Bronk Ramsey, C., Butzin, M., Cheng, H., Edwards, R., Friedrich, M., Grootes, P., Guilderson, T., Hajdas, I., Heaton, T., Hogg, A., Hughen, K., Kromer, B., Manning, S., Muscheler, R., Palmer, J., Pearson, C., van der Plicht, J., Reimer, R., Richards, D., Scott, E., Southon, J., Turney, C., Wacker, L., Adolphi, F., Büntgen, U., Capano, M., Fahrni, S., Fogtmann-Schulz, A., Friedrich, R., Köhler, P., Kudsk, S., Miyake, F., Olsen, J., Reinig, F., Sakamoto, M., Sookdeo, A., Talamo, S., 2020. The IntCal20 Northern Hemisphere Radiocarbon Age Calibration Curve (0-55 cal kBP). Radiocarbon 62, 725–757.
Rhode, D., 2000a. Holocene vegetation in the Bonneville basin. In: Madsen, D.B. (Ed.), Late Quaternary Paleoecology in the Bonneville Basin, vol. 130. Utah Geological Survey Bulletin, Salt Lake City, pp. 149–163.
Rhode, D., 2000b. Middle and late Wisconsin vegetation in the Bonneville basin. In: Madsen, D.B. (Ed.), Late Quaternary Paleoecology in the Bonneville Basin, vol. 130. Utah Geological Survey Bulletin, Salt Lake City, pp. 137–147.
Rhode, D., 2016. Quaternary vegetation changes in the Bonneville basin. In: Oviatt, C.G., Shroder, J.F. (Eds.), Lake Bonneville: A Scientific Update. Developments in Earth Surface Processes, vol. 20. Elsevier, Amsterdam, pp. 420–441.
Rhode, D., Louderback, L.A., 2015. Bonneville basin environments during the Pleistocene-Holocene transition. In: Madsen, D.B., Schmitt, D.N., Page, D. (Eds.), The Paleoarchaic Occupation of the Old River Bed. University of Utah Anthropological Papers No. 128. University of Utah Press, Salt Lake City, pp. 22–29.
Rhode, D., Madsen, D.B., 1998. Pine nut use in the early Holocene and beyond: the Danger Cave archaeobotanical record. J. Archaeol. Sci. 25, 1199–1210.
Rhode, D., Goebel, T., Graf, K.E., Hockett, B.S., Jones, K.T., Madsen, D.B., Oviatt, C.G., Schmitt, D.N., 2005. Latest Pleistocene-early Holocene human occupation and paleoenvironmental change in the Bonneville basin, Utah-Nevada. In: Pederson, J., Dehler, C.M. (Eds.), Interior Western United States: Geological Society of America Field Guide 6. Geological Society of America. https://doi.org/10.1130/2005.fld006(10.
Rhode, D., Madsen, D.B., Jones, K.T., 2006. Antiquity of early Holocene small-seed consumption and processing at Danger Cave. Antiquity 80, 328–339.
Schmitt, D.N., Lupo, K.D., 2012. The Bonneville Estates Rockshelter rodent fauna and changes in late Pleistocene-middle Holocene climates and biogeography in the northern Bonneville basin, USA. Quat. Res. 78, 95–102.
Schmitt, D.N., Lupo, K.D., 2016. Changes in late Quaternary mammalian biogeography in the Bonneville basin. In: Oviatt, C.G., Shroder, J.F. (Eds.), Lake Bonneville: A Scientific Update, Developments in Earth Surface Processes, vol. 20. Elsevier, Amsterdam, pp. 352–370.
Smith, G.M., Barker, P., Hattori, E.M., Raymond, A., Goebel, T., 2013. Points in time: direct radiocarbon dates on Great Basin projectile points. Am. Antiq. 78, 580–594.
Spencer, J.Q.G., Oviatt, C.G., Pathak, M., Fan, Y., 2015. Testing and refining the timing of hydrologic evolution during the latest Pleistocene regressive phase of Lake Bonneville. Quat. Int. 362, 139–145.
Steponaitis, E., Andrews, A., McGee, D., Quade, J., Hsieh, Y., Broecker, W.S., Shuman, B.N., Burns, S.J., Cheng, H., 2015. Mid-Holocene drying of the U.S. Great Basin recorded in Nevada speleothems. Quat. Sci. Rev. 127, 174–185.
Steward, J.H., 1938. Basin-plateau Aboriginal Groups, vol. 120. Smithsonian Institution Bureau of Ethnology Bulletin, Washington, DC.
Surovell, T.A., Brantingham, P.J., 2007. A note on the use of temporal frequency distributions in studies of prehistoric demography. J. Archaeol. Sci. 34, 1868–1877.
Tallavaara, M., Luoto, M., Korhonen, N., Jarvinen, H., Seppa, H., 2015. Human population dynamics in Europe over the last glacial maximum. Proccedings of the National Academy of Sciences 112, 8232–8236.
Thomas, D.H., 2020. Alpine Archaeology of Alta Toquima and the Mt. Jefferson Tablelands (Nevada). Anthropological Papers of the American Museum of Natural History No. 104, New York.
Thompson, R.S., Oviatt, C.G., Honke, J.S., McGeehin, J.P., 2016. Late Quaternary changes in lakes, vegetation, and climate in the Bonneville basin reconstructed from sediment cores from Great Salt Lake. In: Oviatt, C.G., Shroder, J.F. (Eds.), Lake Bonneville: A Scientific Update, Developments in Earth Surface Processes, vol. 20. Elsevier, Amsterdam, pp. 221–291.
Waters, M.R., Stafford Jr., T.W., Carlson, D.L., 2020. The age of Clovis—13,050 to 12,750 cal yr B.P. Science Advances 6, eaaz0455.
Williams, A.N., 2012. The use of summed radiocarbon probability distributions in archaeology: a review of methods. J. Archaeol. Sci. 39, 578–589.
Zdanowicz, C.M., Zielinski, G.A., Germani, M.S., 1999. Mount Mazama eruption: calendrical age verified and atmospheric impact assessed. Geology 27, 621–624.
Zimmerman, S.R.H., Wahl, D.B., 2020. Holocene paleoclimate change in the western US: the importance of chronology in discerning patterns and drivers. Quat. Sci. Rev. 246, 106487.